chemistry

MDPI

Article

Biosynthesis of Copper and Silver Nanoparticles Using *Schinus terebinthifolius* Leaf Extract for Antifungal Activity Against *Fusarium circinatum* and *Pythium tardicrescens*

Mohammed A. A. Elshaer [1], Mervat El-Hefny [2,*], Shimaa E.-S. I. Hassanien [3], Gamal S. Alfawal [1], Waled Abd-Elhamed [4], Mohamed A. M. Abd-Elraheem [1], Abeer A. Mohamed [5], Ayman S. Taha [6] and Tartil M. Emam [7]

1 Agriculture Biochemistry Department, Faculty of Agriculture for Boys, Al-Azhar University, Sadat City 32897, Egypt; mmm_elshaer@azhar.edu.eg (M.A.A.E.); gamalsaleh_elmassry@azhar.edu.eg (G.S.A.); mohamedawad@azhar.edu.eg (M.A.M.A.-E.)
2 Department of Floriculture, Ornamental Horticulture and Garden Design, Faculty of Agriculture (El-Shatby), Alexandria University, Alexandria 21545, Egypt
3 Microbiology, Botany and Microbiology Department, Faculty of Science, Al-Azhar University (Girls Branch), Cairo 11754, Egypt; shiamaa@azhar.edu.eg
4 Agricultural Biochemistry Department, Faculty of Agriculture, Al-Azhar University, Cairo 11651, Egypt; waled.abdelhamed@azhar.edu.eg
5 Plant Pathology Research Institute, Agriculture Research Center (ARC), Alexandria 21616, Egypt; abeera.mohamed81@gmail.com
6 Conservation Department, Faculty of Archaeology, Aswan University, Aswan 81528, Egypt; aymansalahtaha82@yahoo.com
7 Horticulture Department, Faculty of Agriculture, Ain Shams University, Cairo 11241, Egypt; tarteel_emam@agr.asu.edu.eg
* Correspondence: mervat.mohamed@alexu.edu.eg

Abstract

Several bioactive compounds, including phenolic and flavonoid substances, have been identified in the aqueous leaf extract of *Schinus terebinthifolius* (ALE). These compounds are active ingredients in green nanoparticle biosynthesis. Transmission electron microscopy (TEM), energy dispersive X-ray spectroscopy (EDX), zeta potential analysis, and FTIR spectral analysis were used to characterize copper oxide nanoparticles (CuNPs) and silver nanoparticles (AgNPs). According to TEM results, AgNPs exhibited somewhat larger diameters (12 ± 4 nm), were spherical with significant aggregation, and displayed a fairly uniform distribution, while CuNPs were primarily quasi-spherical with a narrow size range of about 4–5 nm. CuNPs showed a much more negative zeta potential value of −25.8 mV, indicating good to high colloidal stability, whereas AgNPs had a zeta potential of −15.5 mV, suggesting moderate stability. The main compounds included chlorogenic acid (10,375.28 µg/g), gallic acid (7015.59 µg/g extract), ellagic acid (1571.29 µg/g extract), and rutin (1485 µg/g extract). The antifungal activity of CuNPs and AgNPs was tested at concentrations of 6, 12, 25, 50, and 75 µg/mL on *Quercus rubra* wood against *Fusarium circinatum* and *Pythium tardicrescens*. The greatest inhibition of *F. circinatum* growth was observed with CuNPs and AgNPs at 75 µg/mL, showing fungal inhibition percentages (FIPs) of 61.48 and 60.74%, respectively. CuNPs and AgNPs at 75 µg/mL exhibited moderate activity against *P. tardicrescens*, with FIPs of 21.48% and 15.92%, respectively. The MICs for AgNPs and CuNPs were 1.5 and 85 µg/mL with *F. circinatum* and *P. tardicrescens*, respectively. Overall, CuNPs and AgNPs demonstrated potential antifungal activity against *F. circinatum* but moderate activity against *P. tardicrescens* compared to the control. This ALE from *S. terebinthifolius* is rich in flavonoids and phenolic compounds, including gallic acid, chlorogenic acid, rutin, ellagic acid, and p-coumaric acid, as identified by HPLC analysis.

Check for updates

Academic Editor: Miguel Jose Yacaman

Received: 7 May 2026
Accepted: 21 May 2026
Published: 26 May 2026

Copyright: © 2026 by the authors. Licensee MDPI, Basel, Switzerland. This article is an open access article distributed under the terms and conditions of the Creative Commons Attribution (CC BY) license.

These biomolecules act as both capping agents, which stabilize the nanoparticles, and reducing agents. Using *S. terebinthifolius* ALE's rich phytochemical profile as a reducing and stabilizing agent provides an environmentally friendly method for the green synthesis of CuNPs and AgNPs.

Keywords: *Schinus terebinthifolius*; leaf aqueous extract; copper nanoparticles; silver nanoparticles; green synthesizes; HPLC; antifungal activity

1. Introduction

Nanotechnology has become one of the most rapidly developing and significant scientific disciplines due to its transformative potential across multiple sectors, including agriculture, industry, environmental protection, and healthcare [1,2]. The ability to manipulate materials at the nanoscale enables the development of systems with enhanced physicochemical and biological properties that are difficult to achieve in their bulk counterparts. In recent years, increasing attention has been directed toward sustainable nanotechnology approaches that minimize environmental impact while maintaining high functional efficiency [3–5].

Among these approaches, the green synthesis of nanoparticles has emerged as a promising alternative to conventional chemical and physical methods. This strategy eliminates the need for hazardous reagents and energy-intensive processes by utilizing biological resources such as plant extracts, microorganisms, and biopolymers as reducing, capping, and stabilizing agents [6,7]. In particular, plant-mediated synthesis offers advantages including simplicity, scalability, cost-effectiveness, and suitability for biological applications [8].

Plant aqueous extracts are rich in bioactive phytochemicals, such as phenolic acids, flavonoids, tannins, terpenoids, alkaloids, proteins, and carbohydrates [9]. These compounds not only facilitate the reduction of metal ions into nanoparticles but also act as stabilizing agents, enhancing nanoparticle stability and biological performance [10,11]. Additionally, many of these phytochemicals possess inherent antioxidant and antimicrobial activities, which may synergistically enhance the bioactivity of the synthesized nanoparticles [12].

One plant of particular interest is *Schinus terebinthifolius* Raddi (Anacardiaceae), commonly known as the Brazilian pepper tree. Its leaves and bark have been widely used in traditional medicine due to their anti-inflammatory, antimicrobial, and healing properties [13,14]. Phytochemical studies have revealed the presence of diverse bioactive compounds, including phenolic acids, flavonoids, tannins, terpenes, and triterpenes [15–20]. Moreover, plant extracts from this species have been successfully utilized in the green synthesis of silver nanoparticles (AgNPs), demonstrating their potential as effective reducing and stabilizing agents [21].

Silver nanoparticles (AgNPs) are among the most extensively investigated nanomaterials due to their broad-spectrum antimicrobial activity and wide-ranging applications in medicine, agriculture, food packaging, and biomedical devices [22,23]. Their antimicrobial efficacy is strongly influenced by physicochemical characteristics such as particle size, shape, and surface chemistry, as well as the nature of the capping agents [24,25]. Green-synthesized AgNPs are particularly advantageous, as their biogenic surface functionalization enhances interaction with microbial cells while reducing cytotoxic effects on non-target organisms [26]. Similarly, copper nanoparticles (CuNPs) have gained attention as cost-effective alternatives to silver-based nanomaterials. CuNPs inhibit microbial

growth through multiple mechanisms, including membrane disruption, protein denaturation, and the generation of reactive oxygen species (ROS) [27,28]. When synthesized via green approaches, CuNPs exhibit improved stability and biocompatibility, supporting their application in agricultural and environmental systems [29].

The antimicrobial activity of metal nanoparticles is generally attributed to their ability to interact with microbial cell surfaces, penetrate cellular membranes, induce oxidative stress, and interfere with essential cellular processes such as DNA replication and enzyme activity [30,31]. Furthermore, phytochemical residues on nanoparticle surfaces can enhance these effects through synergistic interactions [32,33]. These properties make green-synthesized nanoparticles promising candidates for controlling plant pathogens, particularly under increasing concerns of antimicrobial resistance.

In the present work, pine diseases were selected because they cause rapid, widespread mortality in economically vital timber forests and ecosystems, leading to severe economic losses. *Pythium*-induced damping-off is a critical, global issue that causes 25–75% annual plant losses [34]. The disease thrives in high moisture, causing a massive economic impact [35]. Pitch canker disease of pine, also known as pine pitch canker, is a serious threat to pine trees (species in the Pinus genus). Forest ecosystems, including pine plantations, are particularly vulnerable to microbial infections that affect plant health and productivity. Pines are widely distributed, especially in the Mediterranean region, where they play a significant ecological and economic role. However, young pine plants are highly susceptible to infections by fungi, oomycetes, and other pathogens due to their relatively weak protective tissues [36,37]. Among these, diseases such as damping-off caused by *Fusarium circinatum* and *Pythium tardicrescens* are considered highly destructive, leading to significant losses in forest nurseries and plantations [38–41]. Current management strategies are often limited and require intensive intervention, highlighting the need for more sustainable and effective alternatives [42,43].

Despite the growing interest in green-synthesized nanoparticles, few studies have explored the combined use of plant-mediated silver and copper nanoparticles to protect wood materials against phytopathogenic fungi, particularly those affecting forest species such as pine. Therefore, this study aims to synthesize AgNPs and CuNPs using the aqueous leaf extract of *Schinus terebinthifolius* via an eco-friendly approach and to evaluate their antifungal activity on wood samples. This work provides a sustainable strategy for developing long-lasting antifungal agents with potential applications in agriculture and forest protection.

2. Materials and Methods

2.1. Preparation of the Plant Extract

Schinus terebinthifolius Raddi leaves (Figure 1) were collected from trees growing in the nursery of the Department of Floriculture, Ornamental Horticulture and Garden Design, Faculty of Agriculture (El-Shatby), Alexandria University, Alexandria, Egypt. The plant was previously identified at the Department of Forestry and Wood Technology, Faculty of Agriculture, Alexandria University, and a sample was deposited (voucher number Zidan0031).

Schinus terebinthifolius was selected due to its well-documented richness in bioactive phytochemicals, including phenolics, flavonoids, tannins, and terpenoids, which are known to act as effective reducing and stabilizing agents in green nanoparticle synthesis [44,45]. In addition, this plant is widely available and fast-growing and considered an invasive species in several regions, which makes it an economically and environmentally sustainable raw material source. Moreover, previous studies have reported its successful use in the biosynthesis of metallic nanoparticles, supporting its suitability for such applications. Therefore,

its selection is based on both its phytochemical profile and its practical advantages in green synthesis approaches.



Figure 1. The collected *Schinus terebinthifolius* leaves.

Fresh healthy leaves of *S. terebinthifolius* were thoroughly washed with tap water to remove any dust or debris and then chopped and boiled in distilled water for 15–20 min to prepare a clear aqueous leaf extract (ALE), which was then filtered.

2.2. HPLC Conditions

An Agilent 1260 series instrument was used to perform the HPLC analysis of the ALE from *S. terebinthifolius*. A Zorbax Eclipse Plus C8 column (4.6 mm × 250 mm, id, 5 µm film thickness) was used for the separation. Water (A) and 0.05% trifluoroacetic acid in acetonitrile (B) at a flow rate of 0.9 mL/min made up the mobile phase. Using (A) concentrations of 82, 80, 60, 60, 82, 82, and 82%, respectively, a mobile phase linear gradient program was put into place with a step size of 1 min and periods of 5, 8, 12, 15, 16, and 20 min. The multi-wavelength detector was monitored at 280 nm. The injection volume was 5 µL for each sample solution (redissolved in acetone). The column temperature was maintained at 40 °C. Standard HPLC-grade phenolic and flavonoid compounds were used, including gallic acid, chlorogenic acid, catechin, methyl gallate, caffeic acid, syringic acid, pyrocatechol, rutin, ellagic acid, p-coumaric acid, vanillin, ferulic acid, naringenin, rosmarinic acid, daidzein, quercetin, cinnamic acid, kaempferol, and hesperetin. The identification of compounds was confirmed by comparing their retention times with those of the standard compounds. All chemical standards (high-performance liquid chromatography (HPLC grade) were from Sigma-Aldrich (St. Louis, MO, USA) [46]. The HPLC chromatograms of the standard compounds are presented in our recent work [46].

2.3. Synthesis of Copper and Silver Nanoparticles Using Schinus terebinthifolius Aqueous Leaf Extract

2.3.1. Green Synthesis of CuNPs

Copper oxide nanoparticles (CuNPs) were synthesized using the ALE of *S. terebinthifolius*, with slight modifications [47,48]. Separately, a 0.1 M solution of copper sulfate pentahydrate ($CuSO_4 \cdot 5H_2O$) was prepared in distilled water. The leaf extract (10–20 mL) was gradually added to 90–100 mL of the copper salt solution, which was stirred continuously at 60–80 °C for 30–60 min. The color change from light blue to dark brown indicated the formation of CuNPs. The reaction mixture was then allowed to cool to room temperature with continued stirring for 1–2 h to ensure complete reduction and stabilization. The nanoparticles were collected by centrifugation at 4000–5000 rpm for 15–20 min, washed several times with distilled water and ethanol to remove impurities, and dried at 60 °C for 12 h. Optionally,

the dried CuNPs can be calcined at 300–400 °C for 2–3 h to enhance crystallinity, after which they can be stored in an airtight container for further characterization and applications.

2.3.2. Green Synthesis of AgNPs

Silver nanoparticles (AgNPs) were synthesized using the ALE of *S. terebinthifolius*, with slight modifications [49,50]. In brief, a 1 mM solution of silver nitrate ($AgNO_3$) was prepared, and 10 mL of ALE from *S. terebinthifolius* was added to 90 mL of the $AgNO_3$ solution. The mixture was continuously stirred on a hot plate at 60–70 °C for 30–45 min. During this time, the solution gradually changed color from green to dark brown, indicating the formation of AgNPs through the reduction of Ag^+ ions by phenolic and flavonoid compounds present in the ALE. The nanoparticles were then collected by centrifugation at 6000 rpm for 10 min, washed several times with deionized water (ddH_2O) to remove any impurities, and dried in an oven at 50 °C overnight to obtain pure and stable AgNPs suitable for further characterization and applications.

2.4. Characterization of Green Nanometal

2.4.1. Examination by the Transmission Electron Microscopy (TEM)

For transmission electron microscopy (TEM) examination, a small drop of the biosynthesized CuNP and AgNP suspensions obtained using *S. terebinthifolius* ALE was carefully deposited onto carbon-coated copper grids and allowed to dry under ambient conditions. The prepared grids were then examined using a JEOL Plus 1400 transmission electron microscope (JEOL Ltd., Tokyo, Japan) operated at an accelerating voltage of 70 kV. The acquired micrographs were subsequently processed and analyzed using ImageJ software version 1.54r (National Institutes of Health, Bethesda, MD, USA) to determine particle morphology and size distribution [51,52].

2.4.2. Examination by the Energy-Dispersive X-Ray Spectroscopy (EDX)

The elemental composition of the biosynthesized CuNPs and AgNPs produced using the ALE of *S. terebinthifolius* was investigated by energy-dispersive X-ray spectroscopy (EDX). The analysis was carried out using an Oxford INCA 6587 X-ray microanalysis system coupled with a JEOL JSM-5500 LV scanning electron microscope. The measurements were performed at an accelerating voltage of 20 kV to confirm the presence and purity of silver and iron elements in the synthesized nanomaterials and to detect any additional elements originating from phytochemical capping agents [53].

2.4.3. Zeta Potential Analysis

The surface charge and colloidal stability of the biosynthesized CuONPs and AgNPs obtained using the ALE of *S. terebinthifolius* were evaluated through zeta potential measurements. The analysis was performed using a Zetasizer instrument (Malvern Panalytical Ltd., Malvern, UK), which measures the electrostatic potential at the slipping plane of nanoparticles suspended in solution. Zeta potential values provide critical information regarding particle surface charge and dispersion stability, where higher absolute values indicate enhanced repulsive forces and improved stability of the green-synthesized NP suspensions [54,55].

2.4.4. FTIR Examination of the Produced Nanoparticles

FTIR analysis (Shimadzu device, Kyoto, Japan) was used to describe the functional groups of *S. terebinthifolius* ALE and the surfaces of the CuNPs and AgNPs generated by the ALE. This was achieved by carefully scanning an FTIR-type spectrum at a resolution of 4 cm^{-1} within a range of 4000–400 cm^{-1} [56].

2.5. Antifungal Bioassay

The molecularly identified fungal isolates from the diseased root samples from *Pinus halepensis* (Mill.), *Fusarium circinatum* and *Pythium tardicrescens* (Accession numbers PV636492 and PV636491), respectively [43], were used for the antifungal activity. Wood samples prepared at a dimension of 2 × 2 × 2 cm were obtained from *Quercus rubra* L. wood. CuNPs and AgNPs prepared at the concentrations of 6, 12, 25, 50, and 75 µg/mL were applied to these wood samples. All the wood samples were subjected to antifungal evaluation against the growth of the two isolates (*F. circinatum* and *P. tardicrescens*). Three replicates (wood samples) of each concentration for each isolated fungus were used. A total of 100 µL of the produced extract concentration was added to each wood sample.

A two-week-old culture of *F. circinatum* and *P. tardicrescens* on PDA media was prepared. The treated wood samples with the CuNPs and AgNPs, as well as the controls, were inoculated with two fungal discs (0.5 cm diameter) in a Petri dish and then incubated for 7 days at 25 ± 1 °C [43]. The fungal inhibition percentage (FIP) = [(Control growth − Growth in treatment)/Control Growth] × 100, for the treated and untreated woods against each fungus, was measured [57]. The positive control, viz., Cure-M 72% WP (Mancozeb 64% + Metalaxyl 8%), was tested at the recommended dosage (2 g/L) for antifungal activity by the poisoned food technique [58]. Deionized water (ddH_2O) was used as a negative control sample. The minimum inhibitory concentrations (MICs) of the biosynthesized CuNPs and AgNPs by the ALE of *S. terebinthifolius* prepared at concentrations of 1.5 to 85 µg/mL were assessed using the broth dilution method [43,59].

2.6. Statistical Analysis

The percentage of fungal inhibition measured from the treated wood with the concentrated CuNPs and AgNPs (6, 12, 25, 50, and 75 µg/mL) was statistically analyzed using two-way ANOVA (analysis of variance) in SAS software (SAS Institute, Release 8.02, Cary, NC, USA). The mean values of each treatment from the nanoparticles and their concentrations were compared with positive and negative control treatments using Duncan's multiple range test at a 0.05 level of probability.

3. Results

3.1. Chemical Compounds of the Extract by HPLC

Table 1 and Figure 2 present the chemical compounds of the ALE from *S. terebinthifolius* by HPLC analysis. The main compounds were chlorogenic acid (10,375.28 µg/g), gallic acid (7015.59 µg/g extract), ellagic acid (1571.29 µg/g extract), rutin (1485 µg/g extract), p-coumaric acid (838.83 µg/g extract), and methyl gallate (729.88 µg/g extract).

Table 1. Phytochemical compounds identified in the aqueous extract from the leaves of *Schinus terebinthifolius* by HPLC analysis.

Compounds	Area (mAU × s)	Area (%)	Conc. (µg/mL Extract)	Conc. (µg/g Extract)
Gallic acid	1936.38	32.93	140.31	7015.59
Chlorogenic acid	1480.83	25.18	207.51	10,375.28
Catechin	30.28	0.515	7.03	351.54
Methyl gallate	257.49	4.379	14.60	729.88
Caffeic acid	67.41	1.14	4.04	201.76
Syringic acid	1.89	0.032	0.12	6.05

Table 1. *Cont.*

Compounds	Area (mAU × s)	Area (%)	Conc. (µg/mL Extract)	Conc. (µg/g Extract)
Rutin	204.28	3.47	29.70	1485
Ellagic acid	276.39	4.701	31.43	1571.29
p-Coumaric acid	459.41	7.81	16.78	838.83
Vanillin	62.91	1.070	2.13	106.47
Ferulic acid	170.15	2.89	9.84	492.03
Naringenin	49.47	0.841	4.78	239.13
Rosmarinic acid	31.13	0.529	2.77	138.29
Daidzein	2.83	0.048	0.16	8.08
Querectin	7.70	0.131	1.00	49.88
Cinnamic acid	3.07	0.052	0.07	3.32
Kaempferol	8.12	0.138	0.83	41.63

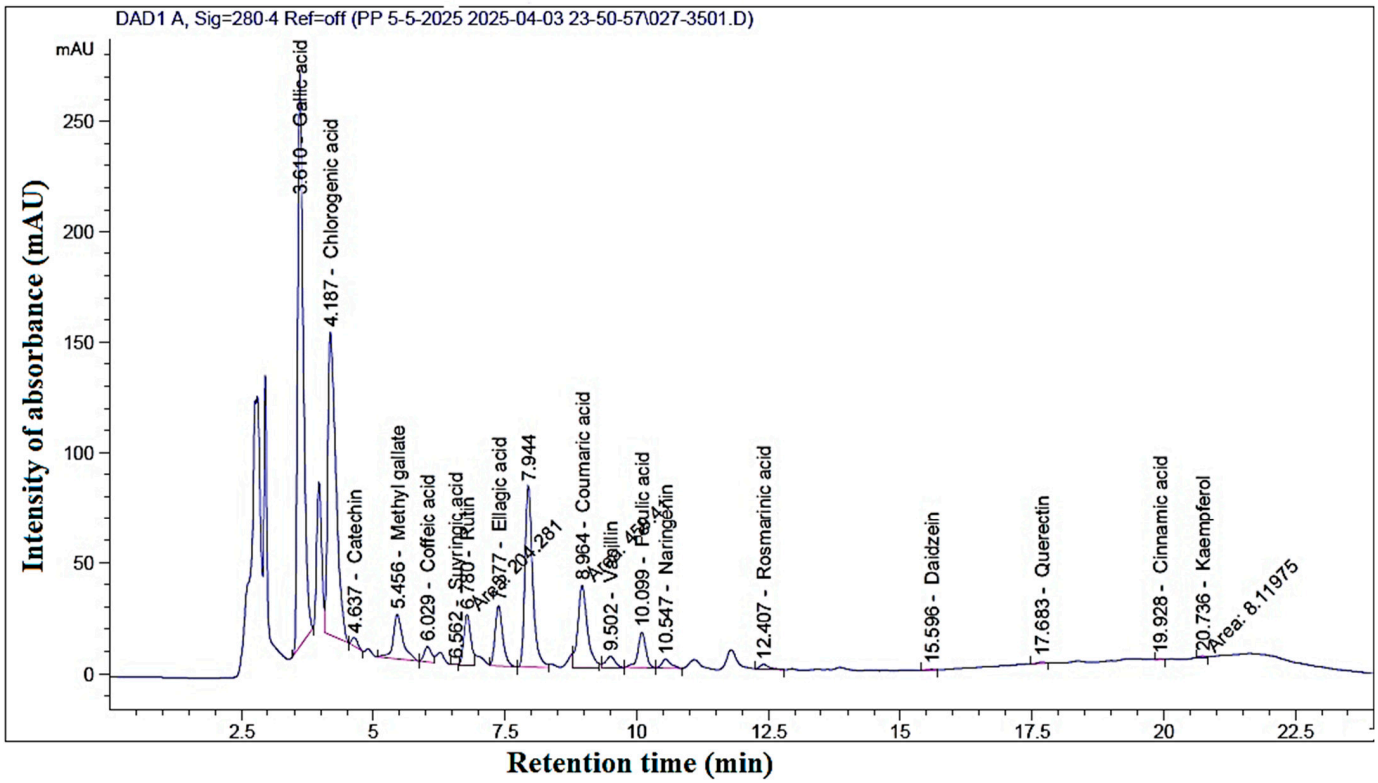


Figure 2. HPLC chromatograms of the identified chemical compounds in the aqueous leaf extract of *Schinus terebinthifolius*.

3.2. Characterization of the Nanomaterials

3.2.1. Transmission Electron Microscopy (TEM)

Transmission electron microscopy (TEM) images revealed that both copper nanoparticles (CuNPs) and silver nanoparticles (AgNPs) synthesized via the green method using the ALE of *S. terebinthifolius* were successfully formed with well-defined nanostructures and good dispersion. For the CuNPs (Figure 3A), the particle sizes ranged from 3.27 to 7.40 nm, with measured diameters of 3.27, 4.09, 4.62, 4.90, 4.90, and 7.40 nm, respectively. The particles were mostly quasi-spherical, exhibiting a narrow size distribution

(predominantly around 4–5 nm). Such an extremely small particle size indicates an efficient bioreduction process facilitated by phytochemicals present in the extract, mainly polyphenols and flavonoids, which acted simultaneously as reducing and capping agents. The fine dispersion and limited aggregation suggest that the phytoconstituents provided strong stabilization through surface functionalization, preventing overgrowth or agglomeration.

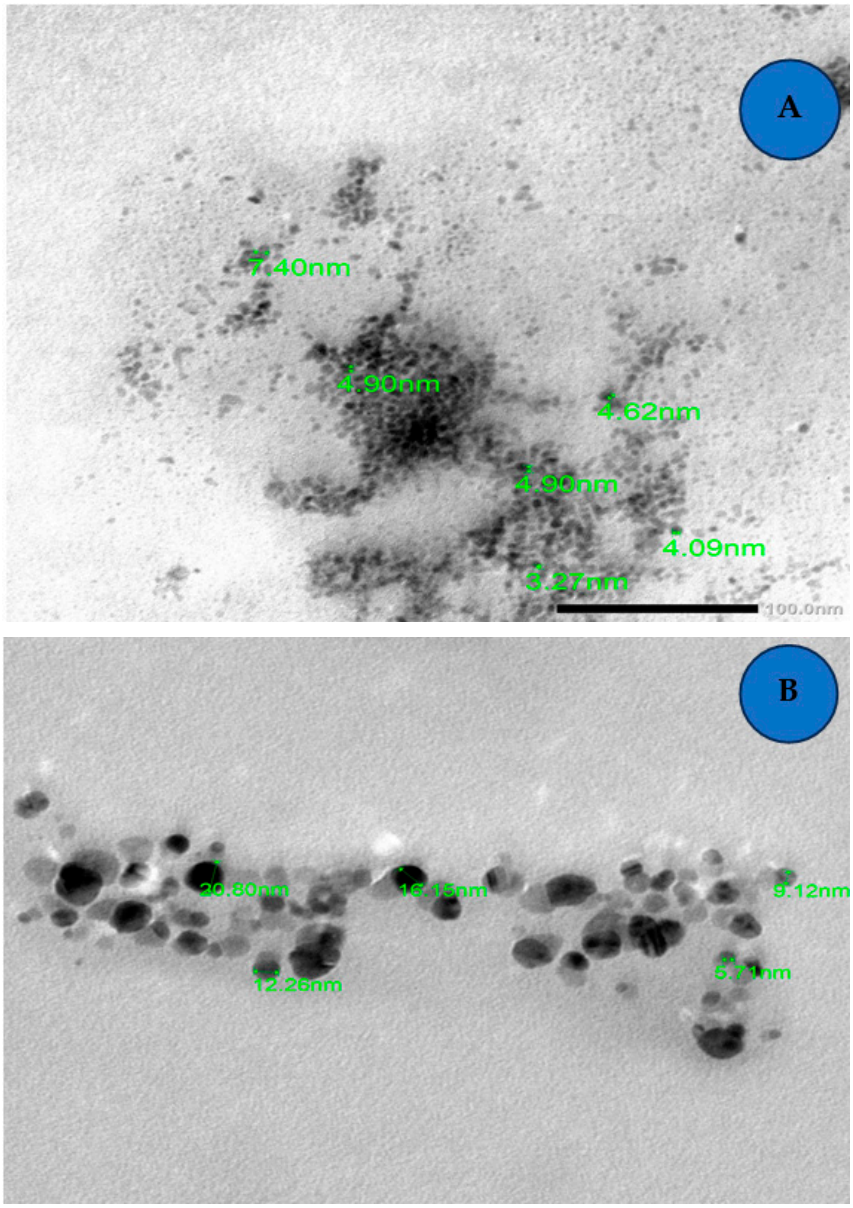


Figure 3. TEM images of (**A**) copper nanoparticles (CuNPs) and (**B**) silver nanoparticles (AgNPs) synthesized using the aqueous leaf extract of *Schinus terebinthifolius*.

In comparison, the AgNPs (Figure 3B) exhibited slightly larger diameters, ranging from 5.71 to 20.80 nm, with specific values of 5.71, 9.12, 12.26, 16.15, and 20.80 nm. The particles appeared predominantly spherical with moderate aggregation and a relatively uniform distribution, showing an average size of approximately 12 ± 4 nm.

3.2.2. EDX Analysis of Green-Synthesized Cu and Ag Nanoparticles Using *Schinus terebinthifolius* Leaf Extract

EDX analysis (Figure 4 and Table 2) confirmed the successful green synthesis of CuNPs (Figure 4a) and AgNPs (Figure 4b) using the ALE of *S. terebinthifolius*. The mass percentage

of the Cu was 4.23% in the biosynthesized CuNPs; moreover, some other elements were found, like K (31.73%), S (3.82%), O (42.89%), and C (16.50%). In the green-synthesized AgNPs, Ag was found at 73.64%, and other elements such as O (17.09%), C (7.08%), and Cl (1.67%) were also reported.

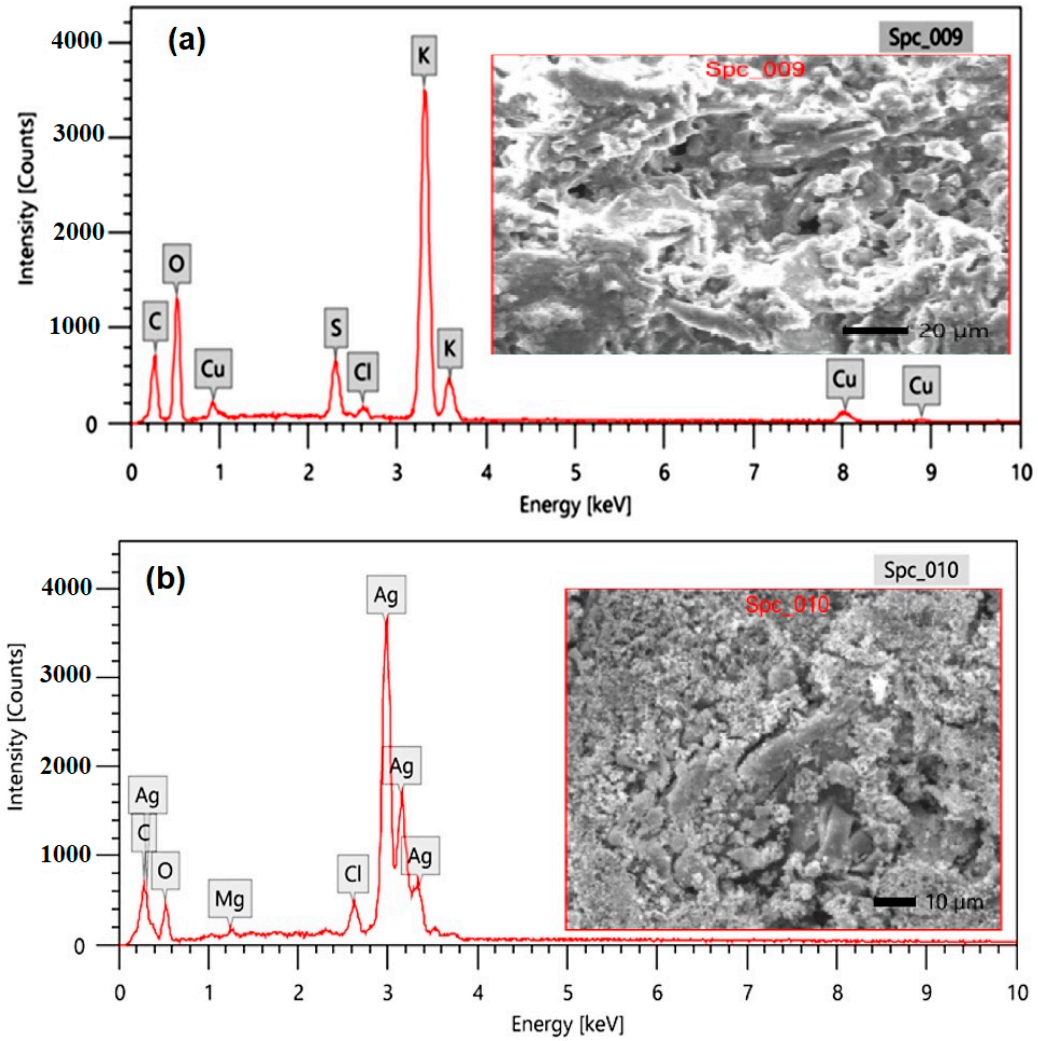


Figure 4. EDX spectrum showing the elemental peaks of (**a**) copper nanoparticles (CuNPs) and (**b**) silver nanoparticles (AgNPs) synthesized using the leaf aqueous extract of *Schinus terebinthifolius*.

Table 2. Elemental composition of copper and silver nanoparticles synthesized using the aqueous leaf extract of *Schinus terebinthifolius* determined by EDX analysis.

CuNPs			AgNPs		
Element	**Mass %**	**Atom%**	**Element**	**Mass %**	**Atom%**
C	16.50 ± 0.14	27.07 ± 0.24	C	7.08 ± 0.08	24.47 ± 0.28
O	42.89 ± 0.45	52.82 ± 0.55	O	17.09 ± 0.33	44.34 ± 0.86
S	3.82 ± 0.07	2.35 ± 0.04	Mg	0.52 ± 0.05	0.89 ± 0.08
Cl	0.83 ± 0.04	0.46 ± 0.02	Cl	1.67 ± 0.06	1.95 ± 0.07
K	31.73 ± 0.22	15.99 ± 0.11	Ag	73.64 ± 0.44	28.34 ± 0.17
Cu	4.23 ± 0.16	1.31 ± 0.05	Total	100.00	100.00
Total	100.00	100.00			

The relatively high K content detected in CuNPs is mainly attributed to the plant extract used in the biosynthesis, which is naturally rich in potassium ions. These ions can remain adsorbed on the nanoparticle surface or be associated with phytochemical capping agents such as phenolics and organic acids. In addition, partial retention of plant-derived residues during purification may contribute to the detected K signal. Therefore, the presence of K is related to the plant-mediated synthesis and surface interactions rather than the copper precursor itself [60–62].

3.2.3. Zeta Potential Analysis of Green-Synthesized CuNPs and AgNPs

Zeta potential analysis (Figure 5) was performed to assess the surface charge and colloidal stability of the green-synthesized CuNPs (Figure 5a) and AgNPs (Figure 5b), prepared using the ALE of *S. terebinthifolius*. The measurements revealed negative zeta potential values for both nanoparticle systems. The zeta potential value of AgNPs was measured at −15.5 mV, suggesting moderate colloidal stability. In contrast, CuNPs exhibited a significantly higher negative zeta potential value of −25.8 mV, reflecting good to high colloidal stability. Values near or exceeding ±25 mV are commonly observed in stable colloidal systems due to strong electrostatic repulsion.

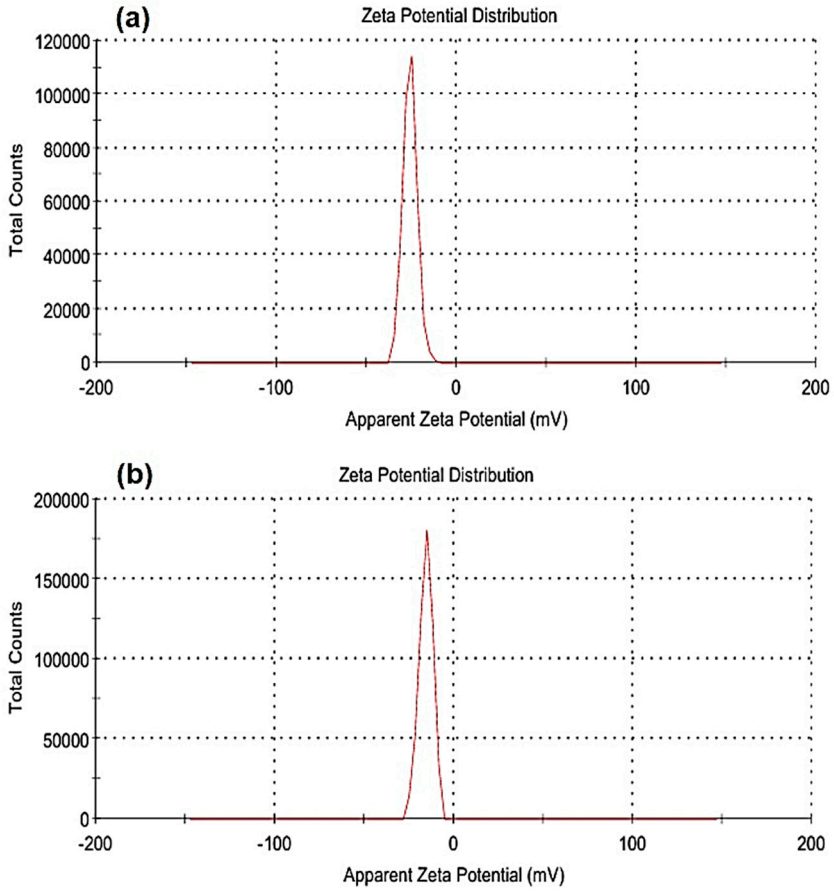


Figure 5. Zeta potential analysis of biosynthesized CuNPs (**a**) and AgNPs (**b**) using *Schinus terebinthifolius* aqueous leaf extract.

3.2.4. FTIR Spectral Analysis

The FTIR spectrum peaks in the ALE from *S. terebinthifolius* correspond to the specific phytochemicals, typically phenolic compounds and flavonoids, responsible for creating and stabilizing the nanoparticles (Figure 6a). The peaks around 3430 cm^{-1} (3883.43, 3868.42, 3586.04 cm^{-1}) correspond to O–H (hydroxyl) and N–H (amine) stretching vibrations, peaks

around 2920 cm^{-1} relate to C–H stretching (alkanes/aliphatic groups), peaks around 1614 cm^{-1} (peaks near 1600–1500 cm^{-1} range) relate to C=C stretching of aromatic rings (flavonoids/phenols), peaks around 1448–1384 cm^{-1} correspond to C–H_2 and C–H_3 bending vibrations (alkanes), and peaks around 1232–1045 cm^{-1} (peaks below 1100 cm^{-1}, e.g., 740.51 and 666.06 cm^{-1}) correspond to C–O stretching (alcohols, carboxylic acids, esters). The presence of these peaks confirms that organic compounds from the *S. terebinthifolius* ALE have successfully coated the surface of the produced nanoparticles.

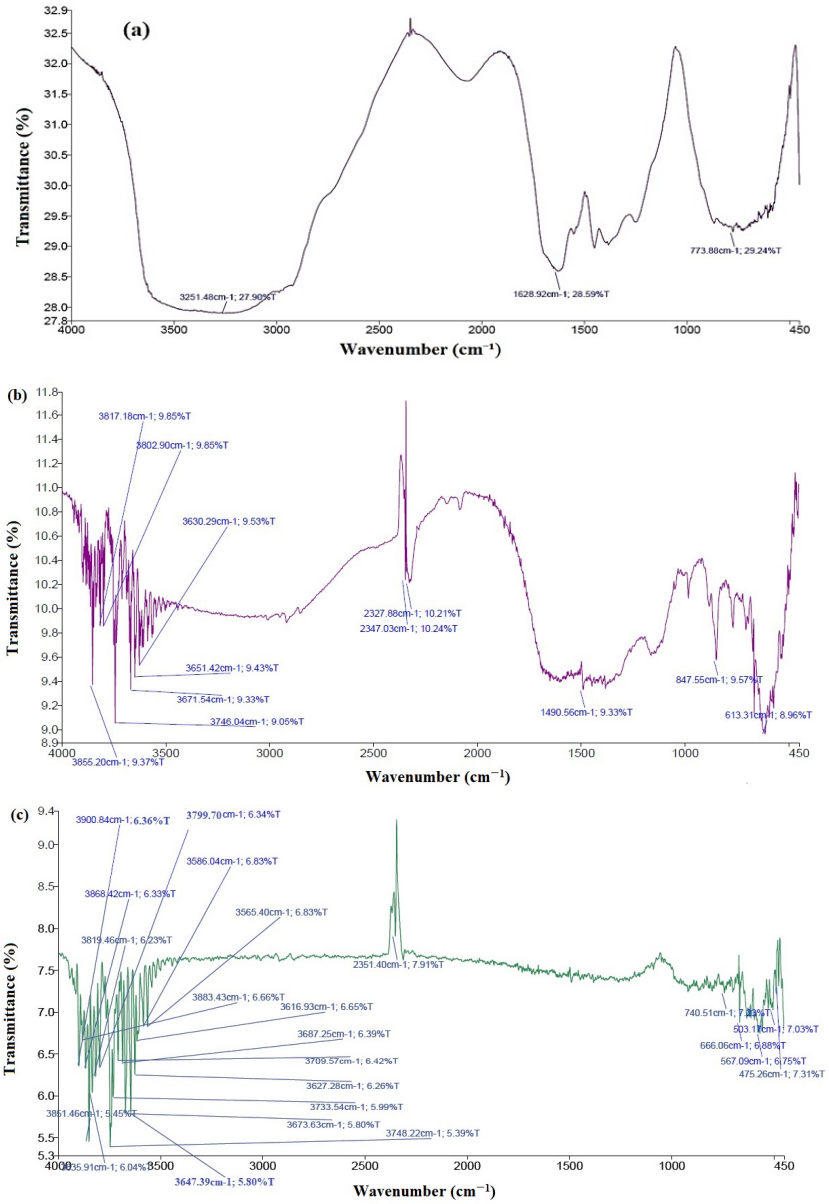


Figure 6. The FTIR spectral analysis of the aqueous leaf extract from *Schinus terebinthifolius* (**a**), the synthesized CuNPs (**b**), and AgNPs (**c**).

The existence of several organic macromolecules is suggested by the significant peaks in CuNPs produced by the ALE of *S. terebinthifolius* (Figure 6b). Peaks at the wavenumber 3200–3500 cm^{-1} (intense peak around this region, e.g., 3422, 3802.90, 3630.29 cm^{-1}) are attributed to the hydroxyl groups of water adsorbed on the nanoparticle surface due to the material's high surface area. Sharp peaks were seen at 3850–3630 cm^{-1}, which usually represent the stretching vibrations of O–H in phenols or alcohols, possibly due to moisture content. The peak around 2920 cm^{-1} is attributed to C–H stretching vibrations

in alkanes or organic acids present in the plant extract, indicating residual organic matter capping the nanoparticles. Peaks in the range of 1600–1640 cm^{-1} are related to C=C or C=O stretching. Peaks in this range (e.g., 1625, 1490.56 cm^{-1}) are usually attributed to C=C stretching vibrations of aromatic rings or carbonyl (C=O) groups from organic components like flavonoids and proteins in the extract. C–O stretching is associated with peaks around 1000–1100 cm^{-1}. In particular, peaks here (e.g., 1033 cm^{-1}) suggest C–O stretching vibrations, which can be connected to the phenolic groups or alcohols from the plant extract that aid in anchoring to the surface of the nanoparticle. The C–N stretching vibration of aromatic amino groups is linked to the peak at 1490 cm^{-1}. Metal–oxygen bonds are characterized by peaks below 1000 cm^{-1} (around 613–846 cm^{-1}). Cu–O stretching vibrations of the bond formation are clearly indicated by peaks at 613.31 and 463 cm^{-1}, which indicate strong evidence for the successful formation of the CuONPs. The reduction of Cu^{2+} ions to Cu/CuONPs and the stabilization of the resulting nanoparticles are caused by these functional groups, which include phenols, flavonoids, and terpenoids found in the *S. terebinthifolius* ALE.

In accordance with the biosynthesized AgNPs by the ALE from *S. terebinthifolius* (Figure 6c), the peaks around 3800–3500 cm^{-1}, 2350 cm^{-1}, 1600 cm^{-1}, and below 1000 cm^{-1} can be summarized to a combination of organic functional groups that are stabilizing the AgNPs. The stretching vibrations of O–H (hydroxyl) groups in alcohols and phenolic compounds, as well as N–H (amine) groups in proteins and amides, are usually attributed to the broad, strong peaks in the ~3880–3200 cm^{-1} area (e.g., 3883, 3819, 3586 cm^{-1}). These are essential for reducing silver ions. The C–H stretching of aliphatic chains (alkanes) found in organic compounds is related to the small peaks at 2900 cm^{-1}. The peak at about 2350 cm^{-1} is probably ambient CO_2 absorption, which is a typical FTIR spectroscopy artifact. C=O stretching in carbonyls (ketones, aldehydes, carboxylic acids, or amides) and C=C stretching in aromatic rings are represented by the peaks in the range 1650–1550 cm^{-1}. These groups are essential for stabilizing and capping the nanoparticles. The C=O (carbonyl) and C=C (aromatic ring) peaks around 1600 cm^{-1} shift when those oxygen atoms coordinate with the metal. The presence of complex organic molecules functioning as stabilizing agents is further confirmed by the "fingerprint region" peaks below ~1100 cm^{-1} (e.g., 740, 666, 567, 475 cm^{-1}), which are linked to different C–O and C–N stretching or C–H bending modes.

3.3. Antifungal Activity

Table 3 and Figure 7 present the antifungal activity of CuNPs and AgNPs on *Quercus rubra* wood against *Fusarium circinatum* and *Pythium tardicrescens*. The highest activity against the growth of *F. circinatum* was observed with the application of CuNPs at 75, 50, and 25 μg/mL, with fungal inhibition percentages (FIPs) of 61.48, 57.04, and 52.22%, respectively. Additionally, AgNPs at 75, 50, and 25 μg/mL showed FIP values of 60.74, 55.18, and 53.33%, respectively.

The application of CuNPs and AgNPs to *Q. rubra* wood showed moderate to weak activity against the growth of *P. tardicrescens*, where the highest activity was found with the treatments of CuNPs at 75 μg/mL, 50 μg/mL, and 25 μg/mL, with values of 21.48, 18.88, and 17.03%. Additionally, AgNPs at the same concentration showed FIP values of 15.92%, 12.59, and 10.37%, respectively.

Overall, CuNPs and AgNPs demonstrated strong antifungal activity against *F. circinatum* but moderate activity against *P. tardicrescens* compared to the control.

Means with the same letter within the same column are not significantly different according to Duncan's multiple range test (PC (positive control): Cure-M 72% WP (Mancozeb 64% + Metalaxyl 8%); NC (negative control): deionized water (ddH_2O)).

Table 3. The antifungal activity of CuNPs and AgNPs against *Fusarium circinatum* and *Pythium tardicrescens*.

Treatment	Concentration	Fungal Inhibition (%)	
		Fusarium circinatum	*Pythium tardicrescens*
PC	2 g/L	56.66 ± 0.00 B *	27.77 ± 0.00 A
NC	ddH_2O	0.00 I	0.00 I
CuNPs	75 µg/mL	61.48 ± 0.64 A	21.48 ± 0.64 B
CuNPs	50 µg/mL	57.04 ± 0.64 B	18.88 ± 0.00 C
CuNPs	25 µg/mL	52.22 ± 0.00 E	17.03 ± 0.64 D
CuNPs	12 µg/mL	48.52 ± 0.64 G	15.55 ± 1.11 E
CuNPs	6 µg/mL	45.18 ± 1.28 H	0.00 I
AgNPs	75 µg/mL	60.74 ± 0.64 A	15.92 ± 0.64 DE
AgNPs	50 µg/mL	55.18 ± 0.64 C	12.59 ± 0.64 F
AgNPs	25 µg/mL	53.33 ± 0.00 D	10.37 ± 1.69 G
AgNPs	12 µg/mL	51.85 ± 0.64 E	8.88 ± 0.00 H
AgNPs	6 µg/mL	49.63 ± 0.64 F	0.00 I

*: Different uppercase letters (A–I) within each column indicate statistically significant differences between treatments (two-way ANOVA, Duncan's multiple range test, $p < 0.05$). Treatments sharing the same letter within the same column are not significantly different. The alphabetical order reflects decreasing antifungal activity from A (highest inhibition) to I (no inhibition).

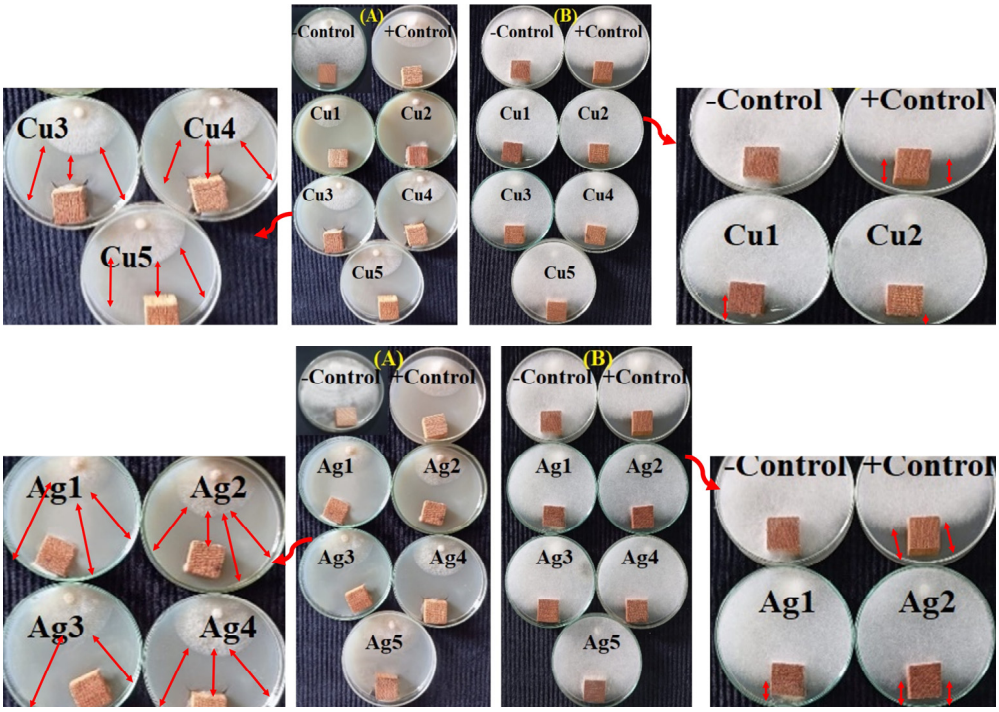


Figure 7. The visual observation of the antifungal activity of CuNPs and AgNPs against the growth of *Fusarium circinatum* (A); *Pythium tardicrescens* (B); Cu1, Ag1; Cu2, Ag2; Cu3, Ag3; Cu4, Ag4; Cu5, Ag5 (75; 50; 25; 12; 6 µg/mL) respectively; +Control (Cure-M); −Control (ddH_2O). Red arrows indicate fungal growth inhibition relative to full growth in the negative control.

4. Discussion

The aqueous leaf extract (ALE) from *Schinus terebinthifolius* was successfully used as a mediated green eco-friendly biosynthesis of CuNPs and AgNPs. Several charac-

terizations confirmed these, e.g., the larger particle size of AgNPs compared to CuNPs can be attributed to the lower reduction potential of Ag^+ ions, allowing more prolonged nucleation and particle growth before stabilization occurs. Nevertheless, the consistent nanoscale dimensions confirm the extract's strong reducing capacity and effective stabilization potential [63,64]. These could be related to the presence of phytochemical compounds in the ALE, including gallic acid, chlorogenic acid, catechin, methyl gallate, caffeic acid, syringic acid, rutin, ellagic acid, p-coumaric acid, vanillin, ferulic acid, naringenin, rosmarinic acid, daidzein, quercetin, cinnamic acid, and kaempferol, which are related to phenolic and flavonoid compounds. *S. terebinthifolius*, widely distributed in tropical and subtropical regions, is known for its rich phytochemical composition. Its leaves have potent antibacterial, antifungal, anti-inflammatory, and antioxidant properties and are rich in phenolic compounds, flavonoids, essential oils, and tannins [15,65]. These characteristics make its ALE an excellent candidate for green synthesis of metal nanoparticles with enhanced biological efficacy. Caffeic acid (5.07 mg/100 mg extract), coumaric acid (1.64 mg/100 mg extract), and syringic acid (1.59 mg/100 mg extract) were the main phenolic chemicals found in the ethanol extract [15]. The polyphenolic chemicals found in the ethyl acetate extract of *S. terebinthifolius* leaves are primarily generated from gallic and ellagic acids [66].

The major compounds in the acetate fraction from the extract were gallic acid, methyl gallate, and 1,2,3,4,6-pentagalloylglucose [67]. The main constituents of the extracts that showed potential antibacterial and antioxidant activity were quercetin, ferulic acid, and caffeic acid [68]. The active EtOAc phase of the EtOH extract from the leaves contained ethyl gallate, methyl gallate, quercitrin, myricetrin, and myricetin [17]. Gallic acid, p-coumaric acid, caffeic acid, and epicatechin were among the phenolic acids and flavonoid chemicals found in the leaf extracts by LC–MS analysis [69].

Numerous active plant compounds with therapeutic or nutritional properties have been used to create nanomaterials. Among these, phenolic acids and flavonoids have received considerable attention due to their potential applications in nanomedicine. The functions of flavonoids as mediators in the formation of metal nanoparticles have recently been reviewed by Sathishkumar et al. [70]. Numerous phenolic acids have also been studied as stabilizers or reducing agents in the production of metal nanoparticles. The uses of phenolic acids as possible mediators for the creation of metal nanoparticles were examined previously [71].

Gallic acid acts as a crucial, eco-friendly agent in the green biosynthesis of nanoparticles, functioning simultaneously as a reducing agent (converting metal ions to metallic nanoparticles) and a capping agent (stabilizing the nanoparticles to prevent aggregation) [72–74]. This dual-action mechanism is driven by its polyphenolic structure, which allows it to donate electrons and subsequently coat the nanoparticle surface, enhancing stability and bioactivity [71]. Gallic acid-coated green-synthesized silver nanoparticles had potent antibacterial action against bacteria and fungi and had minimal damage to healthy cells [71].

For other polyphenolic compounds, hydroxyl groups in the B and C rings of kaempferol are involved in the k-AuNPs formation [75]. Quercetin's carbonyl and hydroxyl groups at places C3 and C5, as well as the catechol group at sites C3′ and C4′, can chelate metal ions to create a variety of metal nanoparticles [76]. It is interesting to note that the study verified that bimetallic Ag-SeNPs mediated by quercetin have greater therapeutic efficacy in terms of antibacterial, antioxidant, and anticancer properties [77].

For the "green" production of metal nanoparticles, such as gold, silver, and copper, chlorogenic acid (CGA) is an efficient natural, environmentally friendly reducing and stabilizing agent that usually results in spherical, stable particles. It functions as a capping agent, improving biocompatibility and inhibiting aggregation for use in antibacterial and

anti-inflammatory treatments [78]. AgNPs were successfully synthesized by CCA with a promising antibacterial functionalization of silk fiber [79]. In order to create stable CuNPs and nanocomposites, CGA isolated from *Prangos serpentinica* extract acts as an environmentally friendly, bioinspired capping and reducing agent. It works by chelating Cu(II) ions, which are then reduced to metallic Cu(0) (usually 20–50 nm) using reagents like sodium borohydride, creating a CGA–Cu(0) matrix for catalytic uses like the Henry reaction [80].

Scampicchio et al. looked into the manufacture of gold nanoparticles using phenolic acids, such as propyl gallate, caffeic acid, protocatechuic acid, ferulic acid, and vanillic acid [81]. Every phytochemical under investigation was capable of reducing gold (III) to gold nanoparticles. The synthesized gold nanoparticles' possible biomedical uses have not yet been examined, though. Zougagh et al. [82] have also investigated sinapinic and syringic acids as possible mediators for the creation of metal nanoparticles. Additionally, caffeic acid has been utilized as a reducing agent in the manufacture of silver and gold nanoparticles [83,84].

The smaller size of CuNPs (3–7 nm) and the spherical, moderately larger AgNPs (5–21 nm) reflect the extract's dual functionality as a natural reducing and stabilizing agent. This highlights the efficiency, simplicity, and sustainability of the green synthesis approach compared with conventional chemical methods, producing NPs that are uniform, stable, and environmentally benign [11,85].

For CuNPs, the spectrum displayed characteristic Cu peaks along with O, C, S, Cl, and K, indicating the presence of both the metallic Cu core and plant-derived organic compounds acting as stabilizing and capping agents [86,87]. The relatively low copper percentage (4.23 wt%) and the high C and K contents suggest that the nanoparticles were effectively coated by phytochemicals, such as flavonoids, phenolics, and organic acids, which prevent aggregation and enhance stability [88,89]. The appearance of S and Cl peaks may be attributed to S- or Cl-containing phytochemicals or natural plant salts, which contribute to the reduction or surface stabilization of the nanoparticles [87]. The presence of O indicates partial surface oxidation, forming a thin CuO/Cu_2O layer, which is responsible for the irregular morphology observed in CuNPs [86,88].

In contrast, the EDX spectrum of AgNPs exhibited strong and distinct peaks of Ag with a high mass percentage (73.6 wt%), confirming the formation of pure metallic silver nanoparticles [90,91]. Minor peaks of C, O, Mg, and Cl correspond to phytochemical residues or mineral components from the extract, participating in reduction and stabilization [91]. The lower oxygen content in AgNPs compared to CuNPs reflects the superior oxidation resistance of Ag, contributing to their more uniform and compact morphology [90].

The elemental composition and SEM micrographs revealed clear differences in morphology and purity between the two samples. AgNPs appeared more uniform and compact, whereas CuNPs exhibited irregular structures due to partial surface oxidation and strong organic capping. These results confirm that *S. terebinthifolius* ALE serves efficiently as both a bioreducing and biostabilizing agent, providing an eco-friendly and effective route for nanoparticle synthesis. The pronounced organic coating in CuNPs and the higher metallic purity in AgNPs highlight the dual functionality of the extract in producing nanoparticles with distinct physicochemical characteristics [92,93].

Although the same ALE was used for the synthesis of both CuNPs and AgNPs, K was detected only in CuNPs. This difference can be explained by the distinct surface chemistry and reactivity of the two metallic nanoparticles rather than any variation in the plant extract. CuNPs exhibit higher surface reactivity and a stronger tendency to interact with oxygen-containing functional groups of phytochemicals, which may facilitate the adsorption or

retention of plant-derived inorganic ions such as K on their surface or in the surrounding organic corona. On the other hand, AgMPs generally form more chemically inert and stable surfaces, which may not favor the adsorption or retention of such residual ions, leading to their absence in the EDX spectrum. Therefore, the presence of K in CuNPs but not in AgNPs reflects differences in metal–surface interactions and capping layer affinity rather than differences in the composition of the plant extract.

The negative zeta potential analysis for both NPs indicates the formation of electrostatically stabilized colloids [54,55]. The negative surface charge in AgNPs is attributed to the adsorption of negatively charged phytochemical constituents from the plant extract onto the nanoparticle surface. Functional groups such as hydroxyl and carboxyl moieties present in polyphenols and flavonoids impart a net negative charge, generating electrostatic repulsion between AgNPs and partially suppressing aggregation. However, zeta potential values in the range of −10 to −20 mV generally indicate limited electrostatic stabilization, which implies that AgNPs may exhibit mild aggregation over extended storage periods [94–96].

The higher negative charge on CuNPs indicates a denser surface coverage by plant-derived stabilizing agents, leading to enhanced charge repulsion and improved dispersion stability in aqueous media [64,97]. A comparative evaluation of both systems demonstrates that CuNPs possess superior colloidal stability compared to AgNPs under identical synthesis conditions. This difference suggests a stronger interaction between the phytochemicals and the copper nanoparticle surface, resulting in a more negatively charged interface. The results clearly confirm the effectiveness of *S. terebinthifolius* ALE as a natural stabilizing agent, capable of producing negatively charged and stable metal nanoparticles via an eco-friendly green synthesis approach [98,99].

Overall, the negative zeta potential values obtained for both AgNPs and CuNPs validate the successful stabilization of the biosynthesized nanoparticles, with CuNPs exhibiting greater electrostatic stability than AgNPs. These findings highlight the potential applicability of the synthesized nanoparticles in biological, environmental, and catalytic systems where colloidal stability is critical.

There is the presence of functional groups that aid in the reduction of Ag^{+} to Ag^{0} and Cu^{2+} ions to Cu^{0} or CuO, and nanoparticle capping agents, which stabilize the resulting nanoparticles and prevent their agglomeration. These were examined by FTIR analysis of the biosynthesized AgNPs, CuNPs, and the ALE of *S. terebinthifolius*. The OH group found in alcohols and phenolic compounds is responsible for the band at 3430 cm^{-1}, according to the analysis of these spectra [100,101]. The band at 1614 cm^{-1} represents the C=C of aromatic rings present in flavonoids and alkaloids, whilst the bands at 2918 and 2921 cm^{-1} are ascribed to the CH group that constitutes the chemical structure of organic groups [102]. The alkanes that comprise the structure of organic compounds are linked to the CH_2 and CH_3 folds, which are represented by the bands at 1448 and 1384 cm^{-1}, respectively [103]. The group C–O found in alcohol, carboxylic acid, ester, and ether is represented by the bands at 1232, 1209, and 1045 cm^{-1} [104].

The shoulder peak at 1626 cm^{-1} in the Khat leaf extract may be caused by conjugated C=O of the proteins that cap and stabilize CuO NPs, C=C stretching, and vibrations about C=O amide [105]. The peaks observed at 613 cm^{-1} and 463 cm^{-1} should be a stretching of Cu-O, which is very close to the results of some previous works [105–107].

These results indicate the presence of some organic compounds that may be related to the process of reduction of Ag^{+} to Ag^{0} and Cu^{2+} ions to Cu^{0} or CuO [105,107–109], resulting in the formation of AgNPs from the proposed biosynthesis process using the ALE of *S. terebinthifolius*, as well as indicating coated AgNPs and CuNPs. It was reported that the high concentration of phenols and flavonoids in the leaf extract facilitates the reduction of copper ions into nanoparticles [110–114].

In accordance with the antifungal activity of the produced nanoparticles, the antifungal activity of CuNPs and AgNPs showed potent activity against *Fusarium circinatum* and weak activity against *Pythium tardicrescens*. Previous works showed that, in addition to their fungistatic action against *Candida albicans* and *Candida glabrata*, AgNPs produced from the ALE of *S. terebinthifolius* showed higher antibacterial efficiency against *Pseudomonas aeruginosa* [100]. This is consistent with the findings of Abd-Elhamed et al. [43], as they demonstrated the influence of both AgNPs and the extract, which were observed to have potential antifungal activities against *P. glomerata*, *F. circinatum*, and *P. tardicrescens*. The activity was achieved at lower concentrations with the synthesized AgNPs. Extracts from leaves of *S. nigrum* exhibited higher antifungal activity against *A. niger*, *A. flavus*, and *C. albicans* as compared to their corresponding aqueous extracts [115].

The synthesized AgNPs by the ALE from *Solanum nigrum* at 75 µg/mL, when applied to *Pinus halepensis* wood, showed fungal inhibition values of 58.14%, 56.66%, and 40.37% against *P. tardicrescens*, *F. circinatum*, and *P. glomerata*, respectively [43].

The biosynthesized AgNPs using a cell-free extract (CFE) of *Bacillus thuringiensis*, prepared at 500 µg/mL, showed antifungal activity against *Aspergillus niger*, *A. terreus*, *A. flavus*, and *A. fumigatus* [116]. In another study, good antifungal activity against *A. niger*, *A. fumigatus*, and *F. soleni* was observed with the application of AgNPs at 50 µg/mL [117]. AgNPs exhibited notable antifungal activity at 47–51 µg/mL against the mycotoxigenic fungi *A. flavus* and *A. ochraceus* [118]. On the other hand, the alcoholic extracts of *S. terebinthifolius* did not exhibit any genotoxic effects on *Aspergillus nidulans* [119]. When evaluating the genotoxic potential of *S. terebinthifolius* extract in an in vitro assay, Carvalho et al. [120] found that, although the extract did not directly break DNA structure, it had the potential to cause oxidative damage to DNA and bacterial mutations.

It should be noted that the selected concentrations for the antifungal assays were based on preliminary screening experiments and previously reported studies on similar biosynthesized nanoparticles, which indicated effective inhibitory activity within this range. The tested range was chosen to ensure adequate dispersion stability of the nanoparticles in the testing medium and to avoid possible aggregation effects that may occur at elevated concentrations, which could influence the reproducibility and interpretation of antifungal results.

Increasing the concentration of nanoparticles can often lead to 100% inhibition, as many studies indicate a concentration-dependent, positive correlation between nanoparticle dosage and inhibition efficiency [121]. Additionally, higher concentrations were not included to maintain a balanced evaluation between efficacy and material usage efficiency. However, the limitation of this study is in not testing higher concentrations, which could provide further insight into the maximum inhibitory potential.

5. Conclusions

An efficient reducing agent for the production of copper and silver nanoparticles was the aqueous extract of *S. terebinthifolius* leaves, demonstrating that green synthesis mediated by plant extracts is straightforward, inexpensive, and environmentally safer, with greater potential. The nanomaterials were well-characterized by means of TEM, EDX, zeta potential, and FTIR analyses. Several bioactive phenolic and flavonoid compounds that are very helpful for phytoreducing agents to produce nanoparticles were identified by HPLC examination of the aqueous extract. The results of antifungal activity showed that the CuNPs and AgNPs, when applied to *Q. rubra* wood, were more effective against *F. circinatum* than *P. tardicrescens*.

Author Contributions: Conceptualization, M.A.A.E. and M.E.-H.; methodology, M.A.A.E., M.E.-H., S.E.-S.I.H., G.S.A., W.A.-E., M.A.M.A.-E., A.A.M. and T.M.E.; M.A.A.E., M.E.-H., S.E.-S.I.H., G.S.A., W.A.-E., M.A.M.A.-E. and A.A.M.; validation, M.A.A.E. and M.E.-H.; formal analysis, M.A.A.E., M.E.-H., S.E.-S.I.H., G.S.A., W.A.-E., M.A.M.A.-E., A.A.M. and T.M.E.; investigation, M.A.A.E., M.A.A.E., M.E.-H., S.E.-S.I.H., G.S.A., W.A.-E., M.A.M.A.-E., A.A.M., A.S.T. and T.M.E.; resources, M.A.A.E., M.E.-H., S.E.-S.I.H., G.S.A., W.A.-E., M.A.M.A.-E., A.A.M., A.S.T. and T.M.E.; data curation, M.A.A.E., M.E.-H. and A.A.M.; writing—original draft preparation, M.A.A.E., M.E.-H. and A.A.M.; writing—review and editing, M.A.A.E., M.E.-H., S.E.-S.I.H., G.S.A., W.A.-E., M.A.M.A.-E., A.A.M., A.S.T. and T.M.E.; visualization, M.A.A.E. and M.E.-H.; supervision, M.A.A.E.; project administration, M.A.A.E.; funding acquisition, M.E.-H. All authors have read and agreed to the published version of the manuscript.

Funding: This research received no external funding.

Data Availability Statement: The original contributions presented in this study are included in the article. Further inquiries can be directed to the corresponding author.

Acknowledgments: The authors would like to thank Mohamed Z.M. Salem, Department of Forestry and Wood Technology, Faculty of Agriculture, Alexandria University, for providing the wood samples to evaluate the antifungal bioassay.

Conflicts of Interest: The authors declare no conflicts of interest.

References

1. Ajaz, M.; Rasool, W.; Mahmood, A. Comprehensive Review of Nanotechnology: Innovations and Multidisciplinary Applications: Comprehensive Review of Nanotechnology. *Futur. Biotechnol.* **2024**, *4*, 12–18. [CrossRef]
2. Zeng, S.; Shakoor, N.; Rui, Y. Nanotechnology and Agricultural Sustainability: A Review. *Nanomaterials* **2025**, *15*, 1755. [CrossRef]
3. Chausali, N.; Saxena, J.; Prasad, R. Nanotechnology as a sustainable approach for combating the environmental effects of climate change. *J. Agric. Food Res.* **2023**, *12*, 100541. [CrossRef]
4. Kodadi, S.K.; Manimekalai, K.; Rabeek, S.M.; Kalme, S.U.; Nathsharma, S.K. Nanotechnology and Green Nanomaterials: Modern Eco-Friendly Sustainable Approach for Combating the Environmental Effects of Climate Change. *Int. J. Environ. Sci.* **2025**, *11*, 238–254. [CrossRef]
5. Salem, M.Z.M.; El-Hefny, M.; Ali, H.M.; Abdel-Megeed, A.; El-Settawy, A.A.A.; Böhm, M.; Mansour, M.M.A.; Salem, A.Z.M. Plants-derived bioactives: Novel utilization as antimicrobial, antioxidant and phytoreducing agents for the biosynthesis of metallic nanoparticles. *Microb. Pathog.* **2021**, *158*, 105107. [CrossRef]
6. Malik, A.Q.; Mir, T.u.G.; Kumar, D.; Mir, I.A.; Rashid, A.; Ayoub, M.; Shukla, S. A review on the green synthesis of nanoparticles, their biological applications, and photocatalytic efficiency against environmental toxins. *Environ. Sci. Pollut. Res.* **2023**, *30*, 69796–69823. [CrossRef] [PubMed]
7. Shahzadi, S.; Fatima, S.; Shafiq, Z.; Janjua, M.R.S.A. A review on green synthesis of silver nanoparticles (SNPs) using plant extracts: A multifaceted approach in photocatalysis, environmental remediation, and biomedicine. *RSC Adv.* **2025**, *15*, 3858–3903. [CrossRef]
8. Saxena, R.; Kotnala, S.; Bhatt, S.C.; Uniyal, M.; Rawat, B.S.; Negi, P.; Riyal, M.K. A review on green synthesis of nanoparticles toward sustainable environment. *Sustain. Chem. Clim. Action* **2025**, *6*, 100071. [CrossRef]
9. Altemimi, A.; Lakhssassi, N.; Baharlouei, A.; Watson, D.G.; Lightfoot, D.A. Phytochemicals: Extraction, isolation, and identification of bioactive compounds from plant extracts. *Plants* **2017**, *6*, 42. [CrossRef]
10. Villagrán, Z.; Anaya-Esparza, L.M.; Velázquez-Carriles, C.A.; Silva-Jara, J.M.; Ruvalcaba-Gómez, J.M.; Aurora-Vigo, E.F.; Rodríguez-Lafitte, E.; Rodríguez-Barajas, N.; Balderas-León, I.; Martínez-Esquivias, F. Plant-based extracts as reducing, capping, and stabilizing agents for the green synthesis of inorganic nanoparticles. *Resources* **2024**, *13*, 70. [CrossRef]
11. Eker, F.; Akdaşçi, E.; Duman, H.; Bechelany, M.; Karav, S. Green synthesis of silver nanoparticles using plant extracts: A comprehensive review of physicochemical properties and multifunctional applications. *Int. J. Mol. Sci.* **2025**, *26*, 6222. [CrossRef] [PubMed]
12. Yazhini, G.; Ilakiya, T.; Shanmugapriya, S.; Durgadevi, D.; Ramasamy, A.; Muthumanickam, K.; Lekshmi, J.K. Phytogenic nanoparticles: A novel strategy for sustainable crop protection. *Plant Stress* **2025**, *18*, 101127. [CrossRef]
13. Martínez, M.J.; Betancourt, J.; Alonso-González, N.; Jauregui, A. Screening of some Cuban medicinal plants for antimicrobial activity. *J. Ethnopharmacol.* **1996**, *52*, 171–174. [CrossRef] [PubMed]

14. de Farias Martorelli, S.B.; Pinheiro, A.L.B.; de Souza, I.A.; Higino, J.S.; Bravo, F. Efeito anti-inflamatório e cicatrizante do extrado de hidroalcoólico de *Schinus terebinthifolius* Raddi (Aroeira) a 30% em orabase-Estudo "In vivo". *IJD. Int. J. Dent.* **2011**, *10*, 80–90.
15. El-Massry, K.F.; El-Ghorab, A.H.; Shaaban, H.A.; Shibamoto, T. Chemical Compositions and Antioxidant/Antimicrobial Activities of Various Samples Prepared from *Schinus terebinthifolius* Leaves Cultivated in Egypt. *J. Agric. Food Chem.* **2009**, *57*, 5265–5270. [CrossRef]
16. Matsuo, A.L.; Figueiredo, C.R.; Arruda, D.C.; Pereira, F.V.; Borin Scutti, J.A.; Massaoka, M.H.; Travassos, L.R.; Sartorelli, P.; Lago, J.H.G. α-Pinene isolated from *Schinus terebinthifolius* Raddi (Anacardiaceae) induces apoptosis and confers antimetastatic protection in a melanoma model. *Biochem. Biophys. Res. Commun.* **2011**, *411*, 449–454. [CrossRef]
17. Ceruks, M.; Romoff, P.; Fávero, O.A.; Lago, J.H.G. Constituintes fenólicos polares de *Schinus terebinthifolius* Raddi (Anacardiaceae). *Química Nova* **2007**, *30*, 597–599. [CrossRef]
18. da Silva, J.H.S.; Simas, N.K.; Alviano, C.S.; Alviano, D.S.; Ventura, J.A.; de Lima, E.J.; Seabra, S.H.; Kuster, R.M. Anti-Escherichia coli activity of extracts from *Schinus terebinthifolius* fruits and leaves. *Nat. Prod. Res.* **2018**, *32*, 1365–1368. [CrossRef]
19. de Lima, M.R.F.; de Souza Luna, J.; dos Santos, A.F.; de Andrade, M.C.C.; Sant'Ana, A.E.G.; Genet, J.-P.; Marquez, B.; Neuville, L.; Moreau, N. Anti-bacterial activity of some Brazilian medicinal plants. *J. Ethnopharmacol.* **2006**, *105*, 137–147. [CrossRef] [PubMed]
20. Rocha, P.d.S.d.; Campos, J.F.; Nunes-Souza, V.; Vieira, M.d.C.; Boleti, A.P.d.A.; Rabelo, L.A.; dos Santos, E.L.; de Picoli Souza, K. Antioxidant and Protective Effects of *Schinus terebinthifolius* Raddi Against Doxorubicin-Induced Toxicity. *Appl. Biochem. Biotechnol.* **2018**, *184*, 869–884. [CrossRef]
21. de Oliveira, D.M.; Menezes, D.B.; Andrade, L.R.; Lima, F.d.C.; Hollanda, L.; Zielinska, A.; Sanchez-Lopez, E.; Souto, E.B.; Severino, P. Silver nanoparticles obtained from Brazilian pepper extracts with synergistic anti-microbial effect: Production, characterization, hydrogel formulation, cell viability, and in vitro efficacy. *Pharm. Dev. Technol.* **2021**, *26*, 539–548. [CrossRef]
22. Almatroudi, A. Unlocking the Potential of Silver Nanoparticles: From Synthesis to Versatile Bio-Applications. *Pharmaceutics* **2024**, *16*, 1232. [CrossRef]
23. Jangra, M.; Saini, G.; Sheoran, P.; Gahlaut, A.; Raj, V. Advances in Silver Nanoparticles: Synthesis, Characterization, and Diverse Applications in Medicine, Environment, Antimicrobial and Antiviral Research. *Crit. Rev. Anal. Chem.* **2025**, 1–25. [CrossRef]
24. Fahim, M.; Shahzaib, A.; Nishat, N.; Jahan, A.; Bhat, T.A.; Inam, A. Green synthesis of silver nanoparticles: A comprehensive review of methods, influencing factors, and applications. *JCIS Open* **2024**, *16*, 100125. [CrossRef]
25. Khalifa, H.O.; Oreiby, A.; Mohammed, T.; Abdelhamid, M.A.A.; Sholkamy, E.N.; Hashem, H.; Fereig, R.M. Silver nanoparticles as next-generation antimicrobial agents: Mechanisms, challenges, and innovations against multidrug-resistant bacteria. *Front. Cell. Infect. Microbiol.* **2025**, *15*, 1599113. [CrossRef]
26. Sidhu, A.K.; Verma, N.; Kaushal, P. Role of Biogenic Capping Agents in the Synthesis of Metallic Nanoparticles and Evaluation of Their Therapeutic Potential. *Front. Nanotechnol.* **2022**, *3*, 801620. [CrossRef]
27. Pourmadadi, M.; Holghoomi, R.; Shamsabadipour, A.; Maleki-baladi, R.; Rahdar, A.; Pandey, S. Copper nanoparticles from chemical, physical, and green synthesis to medicinal application: A review. *Plant Nano Biol.* **2024**, *8*, 100070. [CrossRef]
28. Pellosi, D.S.; Paiva, G.S.; Vital, V.G.; Mendes, A.L.; Santos, N.G.; Kuriki, F.K.; Lira, K.D.; Oliveira, G.C.; Gomes, Y.R.; Lobo, F.G. Harnessing Copper Nanoparticles for Antimicrobial Applications: Advances and Challenges. *Antibiotics* **2025**, *14*, 1170. [CrossRef] [PubMed]
29. Luque-Jacobo, C.M.; Cespedes-Loayza, A.L.; Echegaray-Ugarte, T.S.; Cruz-Loayza, J.L.; Cruz, I.; de Carvalho, J.C.; Goyzueta-Mamani, L.D. Biogenic synthesis of copper nanoparticles: A systematic review of their features and main applications. *Molecules* **2023**, *28*, 4838. [CrossRef]
30. Nisar, P.; Ali, N.; Rahman, L.; Ali, M.; Shinwari, Z.K. Antimicrobial activities of biologically synthesized metal nanoparticles: An insight into the mechanism of action. *JBIC J. Biol. Inorg. Chem.* **2019**, *24*, 929–941. [CrossRef] [PubMed]
31. Makvandi, P.; Wang, C.-Y.; Zare, E.N.; Borzacchiello, A.; Niu, L.-N.; Tay, F.R. Metal-Based Nanomaterials in Biomedical Applications: Antimicrobial Activity and Cytotoxicity Aspects. *Adv. Funct. Mater.* **2020**, *30*, 1910021. [CrossRef]
32. Franco, D.; Calabrese, G.; Guglielmino, S.P.P.; Conoci, S. Metal-based nanoparticles: Antibacterial mechanisms and biomedical application. *Microorganisms* **2022**, *10*, 1778. [CrossRef] [PubMed]
33. Liao, Y.; Wang, X.; Chen, P.; Zhong, Q.; Gong, J. Antimicrobial Mechanisms of Metal-Based Nanomaterials. *Int. J. Nanomed.* **2025**, *20*, 12879–12887. [CrossRef] [PubMed]
34. Karunasinghe, T.G.; Velazhahan, R.; Kazerooni, E.A.; Abdel-Jalil, R.; Al-Sadi, A.M. *Pythium*. In *Compendium of Phytopathogenic Microbes in Agro-Ecology: Vol.1 Fungi*; Amaresan, N., Kumar, K., Eds.; Springer Nature: Cham, Switzerland, 2025; pp. 633–657.
35. Adhikari, A.; Oli, D.; Poudel, P.; Magar, P.; Pandit, S.; Pokhrel, A.; Gurung, S.; Shrestha, J. *Pythium*-induced damping-off disease and its management in tomato (*Solanum lycopersicum* L.): A review. *Agric. Sci. Technol.* **2024**, *16*, 3–17. [CrossRef]
36. Nazarov, P.A.; Baleev, D.N.; Ivanova, M.I.; Sokolova, L.M.; Karakozova, M.V. Infectious Plant Diseases: Etiology, Current Status, Problems and Prospects in Plant Protection. *Acta Naturae* **2020**, *12*, 46–59. [CrossRef] [PubMed]
37. Buttimer, C.; McAuliffe, O.; Ross, R.P.; Hill, C.; O'Mahony, J.; Coffey, A. Bacteriophages and Bacterial Plant Diseases. *Front. Microbiol.* **2017**, *8*, 34. [CrossRef]

38. Elvira-Recuenco, M.; Cacciola, S.O.; Sanz-Ros, A.V.; Garbelotto, M.; Aguayo, J.; Solla, A.; Mullett, M.; Drenkhan, T.; Oskay, F.; Aday Kaya, A.G. Potential interactions between invasive *Fusarium circinatum* and other pine pathogens in Europe. *Forests* **2019**, *11*, 7. [CrossRef]
39. Millar, C.; Buckey, J.; Hagino, R.; Arcaris, S. Spread of pitch canker infections of Monterey pine (*Pinus radiata*) in Cambria, California. *Calif. Ecol. Conserv. Res.* **2024**, *8*, 1–11. [CrossRef]
40. Woodward, S.; Amin, H.; Martín-García, J.; Solla, A.; Diaz-Vazquez, R.; Romeralo, C.; Alves, A.; Pinto, G.; Herron, D.; Fraser, S.; et al. Host-Pathogen Interactions in the Pine-*Fusarium circinatum* Pathosystem and the Potential for Resistance Deployment in the Field. *For. Pathol.* **2025**, *55*, e70020. [CrossRef]
41. Wingfield, M.J.; Hammerbacher, A.; Ganley, R.J.; Steenkamp, E.T.; Gordon, T.R.; Wingfield, B.D.; Coutinho, T.A. Pitch canker caused by *Fusarium circinatum*—A growing threat to pine plantations and forests worldwide. *Australas. Plant Pathol.* **2008**, *37*, 319–334. [CrossRef]
42. Paillet, Y.; Bergès, L.; Hjältén, J.; ÓDor, P.; Avon, C.; Bernhardt-RÖMermann, M.; Bijlsma, R.-J.; De Bruyn, L.U.C.; Fuhr, M.; Grandin, U.L.F.; et al. Biodiversity Differences between Managed and Unmanaged Forests: Meta-Analysis of Species Richness in Europe. *Conserv. Biol.* **2010**, *24*, 101–112. [CrossRef]
43. Abd-Elhamed, W.; Mohamed, A.A.; Saad, Z.H.; Hassanien, S.E.-S.I.; Salem, M.Z.M.; El-Hefny, M. Green synthesis of silver nanoparticles mediated by *Solanum nigrum* leaf extract and their antifungal activity against pine pathogens. *Sci. Rep.* **2025**, *15*, 35025. [CrossRef]
44. Nopkuesuk, N.; Klamrak, A.; Nabnueangsap, J.; Narkpuk, J.; Rahman, S.S.; Saengkun, Y.; Janpan, P.; Soonkum, T.; Sitthiwong, P.; Jangpromma, N.; et al. Hydroethanolic extract of *Schinus terebinthifolia* as a promising source of anti-influenza agents: Phytochemical profiling, cheminformatics, molecular docking and dynamics simulations. *PLoS ONE* **2025**, *20*, e0324990. [CrossRef] [PubMed]
45. da Silva, M.M.; Iriguchi, E.K.; Kassuya, C.A.L.; do Vieira, M.C.; Foglio, M.A.; de Carvalho, J.E.; Ruiz, A.L.T.; de Souza, K.P.; Formagio, A.S. *Schinus terebinthifolius*: Phenolic constituents and in vitro antioxidant, antiproliferative and in vivo anti-inflammatory activities. *Rev. Bras. De Farmacogn.* **2017**, *27*, 445–452. [CrossRef]
46. Salem, M.Z.M.; EL-Shanhorey, N.A.; Mohamed, N.H.; Mohamed, A.A. Phenolic and Flavonoid Compounds from Leaves and Branches of *Schotia brachypetala* for the Development of Biofungicide for Wood Protection. *BioResources* **2025**, *20*, 1069–1087. [CrossRef]
47. Ali, S.G.; Haseen, U.; Jalal, M.; Khan, R.A.; Alsalme, A.; Ahmad, H.; Khan, H.M. Green synthesis of copper oxide nanoparticles from the leaves of *Aegle marmelos* and their antimicrobial activity and photocatalytic activities. *Molecules* **2023**, *28*, 7499. [CrossRef] [PubMed]
48. Andualem, W.W.; Sabir, F.K.; Mohammed, E.T.; Belay, H.H.; Gonfa, B.A. Synthesis of Copper Oxide Nanoparticles Using Plant Leaf Extract of *Catha edulis* and Its Antibacterial Activity. *J. Nanotechnol.* **2020**, *2020*, 2932434. [CrossRef]
49. Kordy, M.G.; Abdel-Gabbar, M.; Soliman, H.A.; Aljohani, G.; BinSabt, M.; Ahmed, I.A.; Shaban, M. Phyto-capped Ag nanoparticles: Green synthesis, characterization, and catalytic and antioxidant activities. *Nanomaterials* **2022**, *12*, 373. [CrossRef]
50. Elshaer, M.A.A.; Abd-Elraheem, M.A.M.; Taha, A.S.; Abo-Elgat, W.A.A.; Abdel-Megeed, A.; Salem, M.Z.M. Green Synthesis of Silver and Ferric Oxide Nanoparticles Using *Syzygium cumini* leaf Extract and Their Antifungal Activity when Applied to Oak Wood and Paper Pulp from *Imperata cylindrica* Grass Biomass. *Waste Biomass Valorization* **2024**, *15*, 6191–6211. [CrossRef]
51. Michen, B.; Geers, C.; Vanhecke, D.; Endes, C.; Rothen-Rutishauser, B.; Balog, S.; Petri-Fink, A. Avoiding drying-artifacts in transmission electron microscopy: Characterizing the size and colloidal state of nanoparticles. *Sci. Rep.* **2015**, *5*, 9793. [CrossRef]
52. Salayová, A.; Bedlovičová, Z.; Daneu, N.; Baláž, M.; Lukáčová Bujňáková, Z.; Balážová, Ľ.; Tkáčiková, Ľ. Green synthesis of silver nanoparticles with antibacterial activity using various medicinal plant extracts: Morphology and antibacterial efficacy. *Nanomaterials* **2021**, *11*, 1005. [CrossRef]
53. Kumar, B.; Smita, K.; Cumbal, L.; Debut, A. Green synthesis of silver nanoparticles using Andean blackberry fruit extract. *Saudi J. Biol. Sci.* **2017**, *24*, 45–50. [CrossRef] [PubMed]
54. Honary, S.; Zahir, F. Effect of zeta potential on the properties of nano-drug delivery systems—A review (Part 2). *Trop. J. Pharm. Res.* **2013**, *12*, 265–273. [CrossRef]
55. Honary, S.; Zahir, F. Effect of zeta potential on the properties of nano-drug delivery systems—A review (Part 1). *Trop. J. Pharm. Res.* **2013**, *12*, 255–264. [CrossRef]
56. Abdellatif, A.A.H.; Alhathloul, S.S.; Aljohani, A.S.M.; Maswadeh, H.; Abdallah, E.M.; Hamid Musa, K.; El Hamd, M.A. Green Synthesis of Silver Nanoparticles Incorporated Aromatherapies Utilized for Their Antioxidant and Antimicrobial Activities against Some Clinical Bacterial Isolates. *Bioinorg. Chem. Appl.* **2022**, *2022*, 2432758. [CrossRef] [PubMed]
57. Elbanoby, N.E.; El-Settawy, A.A.A.; Mohamed, A.A.; Salem, M.Z.M. Phytochemicals derived from *Leucaena leucocephala* (Lam.) de Wit (Fabaceae) biomass and their antimicrobial and antioxidant activities: HPLC analysis of extracts. *Biomass Convers. Biorefinery* **2024**, *14*, 14593–14609. [CrossRef]

58. Erhonyota, C.; Edo, G.I.; Onoharigho, F.O. Comparison of poison plate and agar well diffusion method determining the antifungal activity of protein fractions. *Acta Ecol. Sin.* **2023**, *43*, 684–689. [CrossRef]
59. *CLSI M38-A2*; Reference Method for Broth Dilution Antifungal Susceptibility Testing of Filamentous Fungi; Approved Standard—Second Edition. Clinical and Laboratory Standards Institute (CLSI): Wayne, PA, USA, 2008.
60. Iravani, S. Green synthesis of metal nanoparticles using plants. *Green Chem.* **2011**, *13*, 2638–2650. [CrossRef]
61. Mittal, A.K.; Chisti, Y.; Banerjee, U.C. Synthesis of metallic nanoparticles using plant extracts. *Biotechnol. Adv.* **2013**, *31*, 346–356. [CrossRef]
62. Vanlalveni, C.; Lallianrawna, S.; Biswas, A.; Selvaraj, M.; Changmai, B.; Rokhum, S.L. Green synthesis of silver nanoparticles using plant extracts and their antimicrobial activities: A review of recent literature. *RSC Adv.* **2021**, *11*, 2804–2837. [CrossRef]
63. Antonio-Pérez, A.; Durán-Armenta, L.F.; Pérez-Loredo, M.G.; Torres-Huerta, A.L. Biosynthesis of copper nanoparticles with medicinal plants extracts: From extraction methods to applications. *Micromachines* **2023**, *14*, 1882. [CrossRef] [PubMed]
64. Ashokkumar, M.; Palanisamy, K.; Ganesh Kumar, A.; Muthusamy, C.; Senthil Kumar, K.J. Green synthesis of silver and copper nanoparticles and their composites using *Ocimum sanctum* leaf extract displayed enhanced antibacterial, antioxidant and anticancer potentials. *Artif. Cells Nanomed. Biotechnol.* **2024**, *52*, 438–448. [CrossRef] [PubMed]
65. Oliveira, K.C.; Franciscato, L.M.; Mendes, S.S.; Barizon, F.M.; Gonçalves, D.D.; Barbosa, L.N.; Faria, M.G.; Valle, J.S.; Casalvara, R.F.; Gonçalves, J.E. Essential Oil from the Leaves, Fruits and Twigs of *Schinus terebinthifolius*: Chemical Composition, Antioxidant and Antibacterial Potential. *Molecules* **2024**, *29*, 469. [CrossRef]
66. da Silva Nascimento, M.; dos Santos, P.H.; de Abreu, F.F.; Shan, A.Y.K.V.; Amaral, R.G.; Andrade, L.N.; Souto, E.B.; Santos, M.I.S.; de Souza Graça, A.; Souza, J.B.; et al. *Schinus terebinthifolius* Raddi (Brazilian pepper) leaves extract: In vitro and in vivo evidence of anti-inflammatory and antioxidant properties. *Inflammopharmacology* **2023**, *31*, 2505–2519. [CrossRef]
67. Cavalher-Machado, S.C.; Rosas, E.C.; Brito, F.d.A.; Heringe, A.P.; de Oliveira, R.R.; Kaplan, M.A.C.; Figueiredo, M.R.; Henriques, M.d.G.M.d.O. The anti-allergic activity of the acetate fraction of *Schinus terebinthifolius* leaves in IgE induced mice paw edema and pleurisy. *Int. Immunopharmacol.* **2008**, *8*, 1552–1560. [CrossRef]
68. Uliana, M.P.; Fronza, M.; da Silva, A.G.; Vargas, T.S.; de Andrade, T.U.; Scherer, R. Composition and biological activity of Brazilian rose pepper (*Schinus terebinthifolius* Raddi) leaves. *Ind. Crops Prod.* **2016**, *83*, 235–240. [CrossRef]
69. Chaithep, T.; Muangsanguan, A.; Castagnini, J.M.; Marti-Quijal, F.J.; Sringarm, K.; Arjin, C.; Rachtanapun, P.; Barba, F.J.; Ruksiriwanich, W. Comparative Study on Antioxidant Potential of *Schinus terebinthifolius* Extracts Prepared by Conventional Extraction, Accelerated Solvent Extraction, and Pulsed Electric Field Method. *Molecules* **2025**, *30*, 3589. [CrossRef]
70. Sathishkumar, P.; Gu, F.L.; Zhan, Q.; Palvannan, T.; Mohd Yusoff, A.R. Flavonoids mediated 'Green' nanomaterials: A novel nanomedicine system to treat various diseases—Current trends and future perspective. *Mater. Lett.* **2018**, *210*, 26–30. [CrossRef]
71. Amini, S.M.; Akbari, A. Metal nanoparticles synthesis through natural phenolic acids. *IET Nanobiotechnol.* **2019**, *13*, 771–777. [CrossRef]
72. Mehmood, S.; Kausar Janjua, N.; Tabassum, S.; Faizi, S.; Fenniri, H. Cost effective synthesis approach for green food packaging coating by gallic acid conjugated gold nanoparticles from *Caesalpinia pulcherrima* extract. *Results Chem.* **2022**, *4*, 100437. [CrossRef]
73. Venkatesan, R.; Sivaprakash, P.; Kim, I.; Tawfeek, A.M.; Kim, S.-C. Green synthesis of carbon nanoparticle-reinforced nanocomposites with gallic acid as a crosslinking agent on poly(butylene adipate-co-terephthalate): Preparation, characterization, and performances. *Ind. Crops Prod.* **2024**, *209*, 117949. [CrossRef]
74. Wu, Y.S.; Prasath, A.R.; Mohan, M.; Peroumal, S.; Gopinath, G.R.; Devaraj, D.; Ragavendran, C. Eco-friendly Synthesis of TiO_2 Nanoparticles Utilising Gallic Acid: Structural Characterisation, Broad Spectrum Antibacterial Activity, Antioxidant Assay, and Cytotoxicity of HeLa Cells. *BioNanoScience* **2026**, *16*, 87. [CrossRef]
75. Srinivas Raghavan, B.; Kondath, S.; Anantanarayanan, R.; Rajaram, R. Kaempferol mediated synthesis of gold nanoparticles and their cytotoxic effects on MCF-7 cancer cell line. *Process Biochem.* **2015**, *50*, 1966–1976. [CrossRef]
76. Makarov, V.V.; Love, A.J.; Sinitsyna, O.V.; Makarova, S.S.; Yaminsky, I.V.; Taliansky, M.E.; Kalinina, N.O. "Green" nanotechnologies: Synthesis of metal nanoparticles using plants. *Acta Naturae* **2014**, *6*, 35–44. (In English) [CrossRef] [PubMed]
77. Santos, A.F.; Brotto, D.F.; Favarin, L.R.V.; Cabeza, N.A.; Andrade, G.R.; Batistote, M.; Cavalheiro, A.A.; Neves, A.; Rodrigues, D.C.M.; dos Anjos, A. Study of the antimicrobial activity of metal complexes and their ligands through bioassays applied to plant extracts. *Rev. Bras. De Farmacogn.* **2014**, *24*, 309–315. [CrossRef]
78. Hwang, S.J.; Jun, S.H.; Park, Y.; Cha, S.H.; Yoon, M.; Cho, S.; Lee, H.J.; Park, Y. Green synthesis of gold nanoparticles using chlorogenic acid and their enhanced performance for inflammation. *Nanomedicine* **2015**, *11*, 1677–1688. [CrossRef]
79. Li, L.-L.; Tang, R.-C. A chlorogenic acid mediated synthesis of silver nanoparticles and their application for the antibacterial functionalization of silk fiber. In *Proceedings of the 2017 2nd International Conference on Materials Science, Machinery and Energy Engineering (MSMEE 2017)*; Atlantis Press: Dordrecht, The Netherlands, 2017; pp. 781–784. [CrossRef]
80. Yazdani Sani, N.; Akhlaghi, H.; Motavalizadehkakhky, A. Bio-inspired synthesis of copper nanocatalysts using chlorogenic acid isolated from *Prangos serpentinica* for efficient aqueous-phase Henry reactions. *Discov. Nano* **2026**, *21*, 32. [CrossRef] [PubMed]

81. Scampicchio, M.; Wang, J.; Blasco, A.J.; Sanchez Arribas, A.; Mannino, S.; Escarpa, A. Nanoparticle-Based Assays of Antioxidant Activity. *Anal. Chem.* **2006**, *78*, 2060–2063. [CrossRef]
82. Garcia, M.; Avila, M.; Alfonso, E.; Rios, A.; Zougagh, M. Synthesis of gold nanoparticles using phenolic acids and its application in catalyisis. *J. Mater. Environ. Sci.* **2014**, *5*, 1919–1926.
83. Guo, D.; Dou, D.; Ge, L.; Huang, Z.; Wang, L.; Gu, N. A caffeic acid mediated facile synthesis of silver nanoparticles with powerful anti-cancer activity. *Colloids Surf. B Biointerfaces* **2015**, *134*, 229–234. [CrossRef]
84. Seo, Y.S.; Ahn, E.-Y.; Park, J.; Kim, T.Y.; Hong, J.E.; Kim, K.; Park, Y.; Park, Y. Catalytic reduction of 4-nitrophenol with gold nanoparticles synthesized by caffeic acid. *Nanoscale Res. Lett.* **2017**, *12*, 7. [CrossRef]
85. Stozhko, N.; Tarasov, A.; Tamoshenko, V.; Bukharinova, M.; Khamzina, E.; Kolotygina, V. Green silver nanoparticles: Plant-extract-mediated synthesis, optical and electrochemical properties. *Physchem* **2024**, *4*, 402–419. [CrossRef]
86. Vijayaram, S.; Razafindralambo, H.; Sun, Y.-Z.; Vasantharaj, S.; Ghafarifarsani, H.; Hoseinifar, S.H.; Raeeszadeh, M. Applications of Green Synthesized Metal Nanoparticles—A Review. *Biol. Trace Elem. Res.* **2024**, *202*, 360–386. [CrossRef] [PubMed]
87. Khan, A.; Anas, M.; Ullah, N.; Khattak, W.A.; Ali, M.; Maaza, M.; Shinwari, Z.K. Harnessing green nanotechnology: Exploring the potential of silver, copper, and their nanocomposites for biomedical and agricultural applications. *Pak. J. Bot.* **2025**, *57*, 2197–2220. [CrossRef] [PubMed]
88. Ringu, T.; Das, A.; Ghosh, S.; Pramanik, N. Exploring the potential of copper oxide nanoparticles (CuO NPs) for sustainable environmental bioengineering applications. *Nanotechnol. Environ. Eng.* **2024**, *9*, 679–707. [CrossRef]
89. Gunasena, M.; Galpaya, G.; Abeygunawardena, C.; Induranga, D.; Priyadarshana, H.; Millavithanachchi, S.; Bandara, P.; Koswattage, K. Advancements in Bio-Nanotechnology: Green Synthesis and Emerging Applications of Bio-Nanoparticles. *Nanomaterials* **2025**, *15*, 528. [CrossRef]
90. Rajeshkumar, S.; Bharath, L.V. Mechanism of plant-mediated synthesis of silver nanoparticles—A review on biomolecules involved, characterisation and antibacterial activity. *Chem.-Biol. Interact.* **2017**, *273*, 219–227. [CrossRef]
91. Bahari, A.; Mahdi, M.T.; Katakam, M. Phytosynthesis, characterization of silver nanoparticles using *Pentapetes phoenicea* leaf extract and their antimicrobial effects on some food pathogens. *J. Anal. Sci. Technol.* **2025**, *16*, 30. [CrossRef]
92. Jonuškienė, I.; Narmontaitė, J.; Kantminienė, K.; Tumosienė, I.; Stankevičienė, R.; Petrašauskienė, N. Eco-Friendly Biosynthesis and Characterization of Silver Nanoparticles Using *Zinnia elegans* L. Plant Extracts. *Sustainability* **2025**, *17*, 9451. [CrossRef]
93. Güneş, S.; Ektiren, D.; Vardin, H. Green synthesis and characterization of silver nanoparticles from Gilaburu under varying temperature and pH, with antimicrobial activity and spectral inconsistencies. *Sci. Rep.* **2025**, *15*, 38516. [CrossRef]
94. Dybkova, S.; Goncharuk, O.; Rieznichenko, L.; Terpiłowski, K.; Borysenko, L.; Gruzina, T.; Dybkova, K.; Szewczuk-Karpisz, K. Aqueous dispersions of 'green' silver nanoparticles for eco-applications: Synthesis, structure and biosafety. *J. Mol. Liq.* **2024**, *415*, 126319. [CrossRef]
95. Gecer, E.N. Phytochemistry of *Centaurea saligna*: Silver nanoparticle synthesis, quantification of natural compounds, antioxidant and antibacterial activity. *Sci. Rep.* **2025**, *15*, 26307. [CrossRef]
96. Elmehalawy, N.G.; Zaky, M.M.M.; Eid, A.M.; Fouda, A. Eco-friendly synthesis of silver nanoparticles: Multifaceted antioxidant, antidiabetic, anticancer, and antimicrobial activities. *Sci. Rep.* **2025**, *15*, 37349. [CrossRef]
97. Imtiyaz, A.; Singh, A.; Gaur, R. Comparative Analysis and Applications of Green Synthesized Cobalt Oxide (Co_3O_4) Nanoparticles: A Systematic Review. *BioNanoScience* **2024**, *14*, 3536–3554. [CrossRef]
98. Chaikali, C.; Stola, N.D.; Lampropoulou, P.; Papoulis, D.; Lamari, F.N.; Orkoula, M.; Lykouras, M.; Avgoustakis, K.; Hatziantoniou, S. Green Synthesis and Comparative Analysis of Silver, Copper Oxide, and Bimetallic Ag/CuO Nanoparticles Using *Cistus creticus* L. Extract: Physicochemical Properties, Stability, and Antioxidant Potential. *Int. J. Mol. Sci.* **2025**, *26*, 2518. [CrossRef]
99. Edo, G.I.; Mafe, A.N.; Ali, A.B.M.; Akpoghelie, P.O.; Yousif, E.; Isoje, E.F.; Igbuku, U.A.; Zainulabdeen, K.; Owheruo, J.O.; Essaghah, A.E.A.; et al. Eco-friendly nanoparticle phytosynthesis via plant extracts: Mechanistic insights, recent advances, and multifaceted uses. *Nano TransMed* **2025**, *4*, 100080. [CrossRef]
100. Ferreira, M.D.; Neta, L.C.d.S.; Brandão, G.C.; dos Santos, W.N.L. Evaluation of the antimicrobial activity of silver nanoparticles biosynthesized from the aqueous extract of *Schinus terebinthifolius* Raddi leaves. *Biotechnol. Appl. Biochem.* **2023**, *70*, 1001–1014. [CrossRef] [PubMed]
101. Dev, S.S.; Vineetha, K.; Francis, S. Green synthesis of silver nanoparticles using leaf extract of *Ayapana triplinervis* and its antibacterial activity. *Int. J. Pharm. Sci. Res.* **2018**, *9*, 3897–3902.
102. Vijayakumari, A.; Sinthiya, A. Biosynthesis of phytochemicals coated silver nanoparticles using aqueous extract of leaves of *Cassia alata*–characterization, antibacterial and antioxidant activities. *Int. J. Pharm. Clin. Res.* **2018**, *10*, 138–149.
103. Qais, F.A.; Shafiq, A.; Ahmad, I.; Husain, F.M.; Khan, R.A.; Hassan, I. Green synthesis of silver nanoparticles using *Carum copticum*: Assessment of its quorum sensing and biofilm inhibitory potential against gram negative bacterial pathogens. *Microb. Pathog.* **2020**, *144*, 104172. [CrossRef]
104. Raj, S.; Chand Mali, S.; Trivedi, R. Green synthesis and characterization of silver nanoparticles using *Enicostemma axillare* (Lam.) leaf extract. *Biochem. Biophys. Res. Commun.* **2018**, *503*, 2814–2819. [CrossRef]

105. Gebremedhn, K.; Kahsay, M.H.; Aklilu, M. Green synthesis of CuO nanoparticles using leaf extract of *Catha edulis* and its antibacterial activity. *J. Pharm. Pharmacol.* **2019**, *7*, 327–342. [CrossRef]
106. Sutradhar, P.; Saha, M.; Maiti, D. Microwave synthesis of copper oxide nanoparticles using tea leaf and coffee powder extracts and its antibacterial activity. *J. Nanostruct. Chem.* **2014**, *4*, 86. [CrossRef]
107. Ryntathiang, I.; Vinayakar Senthilkumar, M.; Behera, A.; Dhonthi Shekar, N.; Saravanan, S.; Dharmalingam Jothinathan, M.K.; Kirubakaran, D. Synergistic Synthesis of Copper Nanoparticles via Bioactive Compounds from *Acacia auriculiformis*: Embryonic Toxicology and In Vitro Antioxidant Evaluation. *Biomed. Mater. Devices* **2026**, *4*, 817–832. [CrossRef]
108. Rajkumar, P.V.; Prakasam, A.; Rajeshkumar, S.; Gomathi, M.; Anbarasan, P.M.; Chandrasekaran, R. Green synthesis of silver nanoparticles using *Gymnema sylvestre* leaf extract and evaluation of its antibacterial activity. *S. Afr. J. Chem. Eng.* **2020**, *32*, 1–4. [CrossRef]
109. Benakashani, F.; Allafchian, A.R.; Jalali, S.A.H. Biosynthesis of silver nanoparticles using *Capparis spinosa* L. leaf extract and their antibacterial activity. *Karbala Int. J. Mod. Sci.* **2016**, *2*, 251–258. [CrossRef]
110. da Lurdes Rocha, M.; Dreyer, J.P.; da Silva, M.; Vitali, L.; Assumpção, T.I.; Burin, V.M.; Provenzi, M.A.; Miotto, M.; Affeldt, R.F.; Chaves, E.S. Silver nanoparticles prepared from *Schinus terebinthifolius* extract as new colorimetric sensor for Hg^{2+} determination. *Int. J. Environ. Anal. Chem.* **2025**, *105*, 7635–7655. [CrossRef]
111. Alharbi, M.T.; Al-Rajhi, A.M.; Almuhayawi, M.S.; Gattan, H.S.; Alruhaili, M.H.; Ali, Y.; Selim, S. Nanocomposites of ZnO/CuO/Se Synthesized by *Schinus terebinthifolia* Biomass and their Antioxidant, Cytotoxicity, Anti-H. pylori, and Anti-obesity Properties. *BioResources* **2025**, *20*, 4432. [CrossRef]
112. Santos, C.C.M.; Paixão, P.E.G.; Meneses, J.O.; Dias, J.A.R.; Carvalho, A.S.; dos Santos, H.L.; de Carvalho Batista, T.; Severino, P.; Souto, E.B.; Cardoso, J.C.; et al. Red Aroeira (*Schinus terebinthifolius*)-based zinc oxide nanoparticles: A green approach to combat fish pathogens. *Environ. Toxicol. Pharmacol.* **2026**, *122*, 104946. [CrossRef] [PubMed]
113. dos Reis, R.A.; Oliveira, C.S.; Barbosa, N.S.; Vital, V.G.; da Silva, R.A.G.; de Vasconcellos, S.P.; Cerchiaro, G.; Seabra, A.B. Dual Anticancer and Antibacterial Effects of Green-Synthesized CuO Nanoparticles Mediated by Pink Pepper and Lemongrass Essential Oils. *BioNanoScience* **2026**, *16*, 93. [CrossRef]
114. Kandav, G.; Sharma, T. Green synthesis: An eco friendly approach for metallic nanoparticles synthesis. *Part. Sci. Technol.* **2024**, *42*, 874–894. [CrossRef]
115. Katsura, H.; Tsukiyama, R.-I.; Suzuki, A.; Kobayashi, M. In Vitro Antimicrobial Activities of Bakuchiol against Oral Microorganisms. *Antimicrob. Agents Chemother.* **2001**, *45*, 3009–3013. [CrossRef]
116. Hashem, A.H.; Saied, E.; Amin, B.H.; Alotibi, F.O.; Al-Askar, A.A.; Arishi, A.A.; Elkady, F.M.; Elbahnasawy, M.A. Antifungal activity of biosynthesized silver nanoparticles (AgNPs) against *Aspergilli* causing aspergillosis: Ultrastructure Study. *J. Funct. Biomater.* **2022**, *13*, 242. [CrossRef]
117. Khan, T.; Yasmin, A.; Townley, H.E. An evaluation of the activity of biologically synthesized silver nanoparticles against bacteria, fungi and mammalian cell lines. *Colloids Surf. B Biointerfaces* **2020**, *194*, 111156. [CrossRef] [PubMed]
118. Khalil, N.M.; Abd El-Ghany, M.N.; Rodríguez-Couto, S. Antifungal and anti-mycotoxin efficacy of biogenic silver nanoparticles produced by *Fusarium chlamydosporum* and *Penicillium chrysogenum* at non-cytotoxic doses. *Chemosphere* **2019**, *218*, 477–486. [CrossRef]
119. Ruiz, A.R.; De la Torre, R.A.; Alonso, N.; Villaescusa, A.; Betancourt, J.; Vizoso, A. Screening of medicinal plants for induction of somatic segregation activity in *Aspergillus nidulans*. *J. Ethnopharmacol.* **1996**, *52*, 123–127. [CrossRef]
120. Carvalho, M.G.; Freire, F.D.; Raffin, F.N.; Aragão, C.F.S.; Moura, T.F.A.L. LC Determination of Gallic Acid in Preparations Derived from *Schinus terebinthifolius* Raddi. *Chromatographia* **2009**, *69*, 249–253. [CrossRef]
121. AlHarethi, A.A.; Abdullah, Q.Y.; AlJobory, H.J.; Anam, A.M.; Arafa, R.A.; Farroh, K.Y. Zinc oxide and copper oxide nanoparticles as a potential solution for controlling *Phytophthora infestans*, the late blight disease of potatoes. *Discov. Nano* **2024**, *19*, 105. [CrossRef] [PubMed]

Disclaimer/Publisher's Note: The statements, opinions and data contained in all publications are solely those of the individual author(s) and contributor(s) and not of MDPI and/or the editor(s). MDPI and/or the editor(s) disclaim responsibility for any injury to people or property resulting from any ideas, methods, instructions or products referred to in the content.